(NASA-CR-158705)   COMETARY PARTICULATE          N79-25959
ANALYZER   Final Report (TRW Defense and
Space Systems Group)   56 p HC A04/MF A01
                                      CSCL 03B        Unclas
                                             G3/91   15376

# COMETARY PARTICULATE ANALYZER

## FINAL REPORT

Prepared for

NASA Headquarters

Washington, D.C. 20546

CONTRACT NASW-3151

MAY 1979

**TRW**
DEFENSE AND SPACE SYSTEMS GROUP

One Space Park • Redondo Beach • California

# COMETARY PARTICULATE ANALYZER

## FINAL REPORT

Prepared for

NASA Headquarters
Washington, D.C. 20546

CONTRACT NASW-3151

May 1979

Prepared by

J. F. Friichtenicht     (213)536-1453
D. J. Miller            (213)535-0547
N. G. Utterback         (213)536-1453

Principal Investigator:  *J. F. Friichtenicht*
J. F. Friichtenicht

**TRW**
DEFENSE AND SPACE SYSTEMS GROUP

One Space Park ● Redondo Beach ● California

## ABSTRACT

A preliminary experimental and analytical evaluation of a concept for determining the relative abundance of elements contained in cometary particulates has been conducted with very encouraging results. The technique utilizes a short ($\sim$ 10 ns) high intensity ($10^9$ - $10^{10}$ watts cm$^{-2}$) burst of laser radiation to vaporize and ionize collected particulate material. Ions extracted from this laser produced plasma are analyzed in a time of flight mass spectrometer to yield an atomic mass spectrum representative of the relative abundance of elements in the particulates. Critical aspects of the development of this system are determining the ionization efficiencies for various atomic species and achieving adequate mass resolution. A literature survey revealed and limited experimental results indicate that the range of ionizing efficiencies is within reasonable bounds. The thermal energy spread within the high temperature plasma tends to limit the mass resolution. However, a technique called energy-time focus utilizes static electric fields to alter the length of the ion flight path in proportion to the ion initial energy. This results in a corresponding compression in the range of ion flight times which effectively improves the inherent resolution. Sufficient data were acquired to develop preliminary specifications for a flight experiment. Additional experiments are required to demonstrate the full capability of the instrument.

# CONTENTS

COMETARY PARTICULATE ANALYZER

1.  INTRODUCTION

This report summarizes the experimental and analytical work conducted under NASA Contract No. NASW-3151 for the period from 1 September 1978 to 03 May 1979.  The overall objective of the program was to assess the feasibility of the Cometary Particulate Analyzer (CPA) concept for the in situ determination of the elemental composition of particulates released from a comet nucleus.  Characterization of the physical and chemical properties of these particulates is one of the major scientific objectives of the Halley flyby-Tempel 2 rendezvous mission currently under consideration by NASA.

In the CPA concept, collected particulates are reduced to a high temperature plasma by irradiation with a short pulse of high intensity laser light.  Ions are extracted from the plasma by application of an electric field at the particulate collector surface.  The extracted ions are accelerated by the same electric field to a fixed kinetic energy and are subsequently analyzed in a time of flight ion mass spectrometer.  The raw data from the CPA gives the relative number of ions as a function of atomic weight.  In principle, the accelerated ion stream contains ions of all of the elemental species present in the particle including normally volatile fractions.  The degree of ionization of a given atomic species depends upon its ionization potential and the temperature of the plasma.  In practice, the plasma temperature must be high enough to ionize a significant fraction of the high ionization potential atomic species expected to be present in the particulates.  At these temperatures, the number of molecular ions present in the plasma is expected to be vanishingly small.  We expect that it will be a relatively simple matter to determine the relative abundance of all of the significant elements contained in the particle.  Giving the relative elemental abundances, it may be possible to reconstruct the mineralogical structure of the particulates.

The combination of laser blow-off ionization and time of flight (TOF) mass spectrometry that comprises the CPA was arrived at after careful consideration of other techniques for accomplishing either or both of the

1

necessary functions. We believe for a variety of reasons, some fundamental and some practical, that the CPA is a strong candidate for the eventual flight experiment. Based partially on our work and partially on the work of others as reported in the literature, we believe that the CPA is potentially capable of unambiguously specifying the relative abundances of all elements (including condensed volatile material) contained in the collected particles over the atomic mass range from 1 to 60 amu. The arguments in support of this belief are delineated in the balance of this report.

The following section briefly describes the CPA concept for the purpose of identifying the critical issues that must be resolved in order to establish the feasibility of the approach. Section 3 describes the experimental measurements conducted under the current program and summarizes their significance. In Section 4 we describe the concept of "energy focus" which is a technique for improving the mass resolution of the CPA. The requirement for energy focus will become clear in the discussion preceding its description. Section 5 contains our current best estimate of some of the specifications of a flight experiment that will yield the results described above. In Section 6, a brief summary of the accomplishments of the current program is given. Finally, a synopsis of related work by other experimenters is presented in the Appendix.

## 2. CPA CONCEPTUAL DESCRIPTION

### 2.1 PRINCIPLES OF OPERATION

Figure 2-1 is a sketch of the simplest CPA configuration. The particles to be analyzed are assumed to be at rest on the surface of a collector that has been retracted from a region exposed to the particulate flux to the position indicated in the sketch. (Implementation of the required manipulation of the collector, its geometric form, and the material from which the collector is fabricated were not evaluated in any detail during the course of this study.) The collector is maintained at a positive potential relative to spacecraft ground by a low-current power supply. A grounded planar grid mounted parallel to the collector surface and a distance $L_1$ from it establishes an electric field between the collector and the grid.

Irradiation of the collector surface with a focused, high intensity burst of laser light converts a thin layer of the material within the laser spot into a highly ionized plasma. Due to high internal pressure, the plasma bubble begins to expand into the surrounding vacuum. As the plasma density begins to drop because of the expansion process, the applied electric field extracts ions from the plasma and accelerates them across the gap between the collector and the grounded grid.

Neglecting for the moment any thermal velocity derived from the hot plasma, the velocity of an ion upon reaching the plane of the grid is

$$v = \left(\frac{2qV}{m}\right)^{1/2} \text{ m sec}^{-1} \tag{2.1}$$

where $V$ is the voltage difference between the collector plate and the grid and $q/m$ is the charge to mass ratio of the ion. Upon passing through the grid, the ions enter a field free region where they drift at constant velocity to an ion detector located at a distance $L_2$ from the accelerator grid. The time interval required for an ion to traverse the distance from the collector to the ion detector is given by

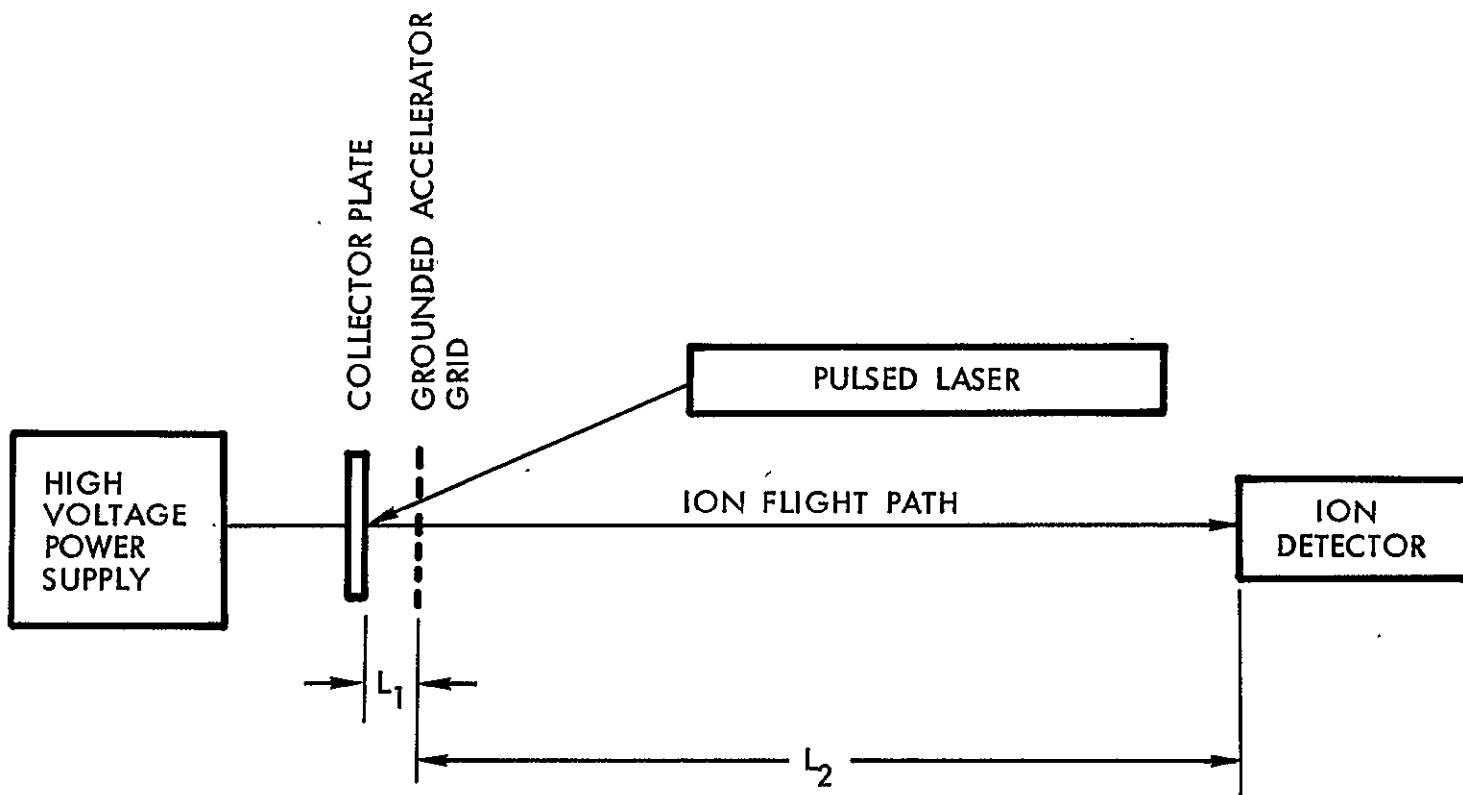$$t = L\left(\frac{m}{2qV}\right)^{1/2} \text{ sec} \tag{2.2}$$

3

Figure 2-1. Conceptual Cometary Particulate Analyzer.

where $L = L_1 + L_2$. The difference in arrival times of two ion groups with atomic masses $m_1$ and $m_2$ with $m_2 > m_1$ is given by

$$\Delta t = \frac{L}{v^{1/2}} \left(0.72 \times 10^{-4}\right)\left(m_2^{1/2} - m_1^{1/2}\right) \text{ sec} \qquad (2.3)$$

where MKS units have been assumed.

Thus, this approach segregates the various mass ions by their arrival time at the detector. A recording of the time-dependent ion current yields a mass spectrum of the plasma ions where the relative magnitude of the ion current peaks is related to the relative abundance of ions in the plasma.

This idealized description of the CPA serves to identify some of the reasons for choosing this particular approach to the analysis of cometary particles, specifically;

1. The output signal for a given "event" includes the entire atomic mass range of interest.

2. Weight and power demands are minimal, requiring only a low average current high voltage supply and a long enough drift distance to yield the desired resolution.

3. The system requires only a single ion detector and associated electronics.

## 2.2 FACTORS AFFECTING CPA PERFORMANCE

### 2.2.1 Atomic Mass Resolution

Equation 2.2 shows that there is a unique relationship between the charge to mass ratio of an ion and its transit time through the time-of-flight range. In practice, however, several effects combine to produce a smearing in the arrival time at the ion detector. This causes a finite width of the ion pulses and has the potential of degrading the effective resolution of the instrument. The resolution may be defined as the ratio of the mean time of arrival of a group of ions with a given charge-to-mass to the time width of the ion pulse. For the idealized case discussed above, the pulse width is zero and the resolution infinite.

One of the factors contributing to a finite pulse width is the time interval over which ions are extracted from the plasma. This time interval

5

will likely be on the order of the laser pulse duration. If this is the case, the difference in the arrival times of two ion groups must be greater than the laser pulse duration for the two ion groups to be resolved, i.e., $t_L \leq \Delta t$ where $t_L$ is the laser pulse duration. Utilizing this relationship in Equation 2.3 yields an upper limit for the accelerating voltage given by

$$V_{max} \leq \left(\frac{L}{t_L}\right)^2 0.518 \times 10^{-8} \left(m_2^{1/2} - m_1^{1/2}\right)^2 \text{ volts} \quad . \quad (2.4)$$

Figure 2-2 gives the maximum accelerating voltage as a function of $m_2$ for two values of $t_L$. Here we have arbitrarily chosen L = 0.5 meter and have defined $m_1 = m_2-1$ meaning that the indicated voltage for a given value of $m_2$ results in resolution of the $m_1$ and $m_2$ ion peaks.

Another factor that may affect the width of the ion pulses is the time interval over which ions are extracted from the plasma even if the time required to form the plasma is small. Efficient extraction can occur only when the applied electric field dominates the space charge forces tending to maintain charge neutrality. If we treat the accelerator region as a planar diode with ions extracted from the heated spot on the anode, the space charge limited ion current density is given by the expression

$$J_+ = \frac{\varepsilon_0}{2.25} \left(\frac{2q}{m}\right)^{1/2} \frac{V^{3/2}}{L_1^2} \text{ amps cm}^{-2} \quad\quad (2.5)$$

where $\varepsilon_0$ is the permittivity of free space. For singly charged silicon ions, for example, the maximum current density is

$$J_{Si+} = 1.03 \times 10^{-8} \frac{V^{3/2}}{L_1^2} \text{ amps cm}^{-2} \quad\quad (2.6)$$

For illustrative purposes, assumed values of V = 2000 volts and $L_1$ = 1 cm gives a maximum Si ion current density of $0.92 \times 10^{-3}$ amps cm$^{-2}$. For a laser spot size of 0.03 cm diameter, the total current that can be transported across the diode is $6.5 \times 10^{-7}$ amperes. For a time interval of 50 nsec, the total charge that can be transported is $3.25 \times 10^{-14}$ coulombs.

Although these assumed conditions are somewhat unrealistic, the calculations convincingly illustrate the importance of space charge forces
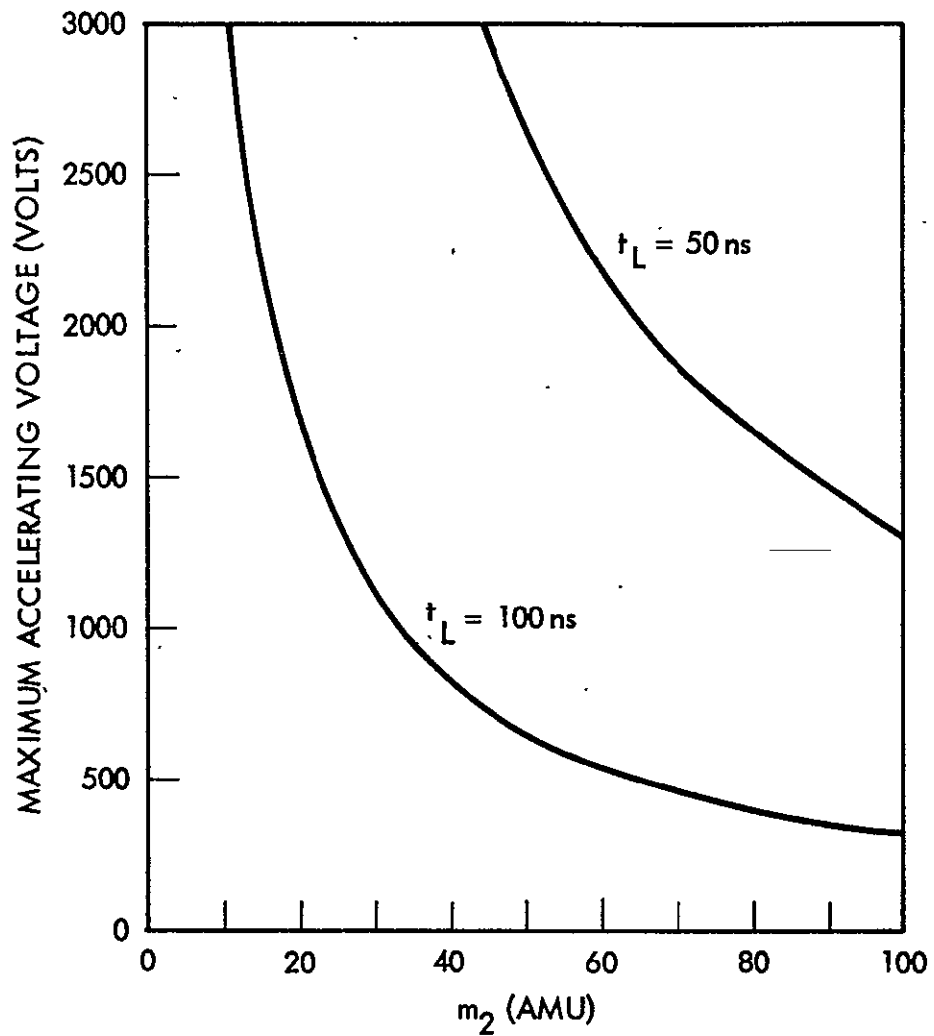
6

Figure 2.2.  Maximum accelerating voltage resulting in
resolution of the ion peaks corresponding to
masses $m_2$ and $m_2-1$ for two values of laser
pulse duration.  A TOF distance of 0.5 M was
chosen.

7

on charge extraction from the plasma. Further, they show that the total amount of charge produced by the laser bombardment has an upper limit. In practice, values of the current density, total ion current, and integrated charge are probably lower limits due to the dynamic nature of the plasma. Some degree of radial expansion of the ions can be tolerated which has the effect of increasing the area of the diode. The plasma can expand into the diode space effectively decreasing the diode separation. Finally, ions within the plasma have a finite thermal energy. All of these factors combine to increase the ion current that can be extracted from the plasma and transported across the space. Experiments conducted during this program have shown that satisfactory conditions can be achieved. The experiments have also shown that the production of excess ionization does affect the resolution and, in extreme cases, the plasma can penetrate to the grid causing an arc to form across the accelerating region.

Another factor that contributes to broadening of the individual ion peaks is the variation in initial energy of the ions. Equation 2.2 tacitly assumes that $v_0 = 0$. More realistically there will be a range of initial velocities in the plasma due to the high plasma temperature. The range encompasses zero at one extreme and some sensible upper limit where the fraction of ions with velocities in excess of the upper limit is small enough to be ignored. The drift velocity of an ion with an initial energy $E_0$ after acceleration through a potential difference V is

$$v = \left[\frac{2}{m}(E_0 + qV)\right]^{1/2} \text{ m sec}^{-1} \quad . \qquad (2.7)$$

The transit time to the detector in the time of flight range is given by

$$t = \frac{L}{\left[\frac{2q}{m} V (1 + k)\right]^{1/2}} \text{ sec} \qquad (2.8)$$

where $L = 2L_1 + L_2$ as before and it is assumed that $L_1 << L_2$. Also, in Equation 2.8, the initial energy has been given as a fraction of the energy imparted to the ion by the applied electric field, i.e. $E_0 = kqV$. For illustrative purposes, let us consider the effect on the arrival time of two ion groups of masses $m_2$ and $m_1$ with $m_2 > m_1$ when a range of initial

8

velocities exists. Ignoring the effect of a finite pulse duration, the latest arriving ions with mass $m_1$ are those with zero initial energy. The earliest arriving ions with mass $m_2$ are those with the maximum initial kinetic energy. In order to resolve the two groups we require that the latest time of arrival of the mass $m_1$ ions be less than the transit time of the fastest mass $m_2$ ion, i.e.

$$\frac{L}{\left[\frac{2qV}{m_1}\right]^{1/2}} \leq \frac{L}{\left[\frac{2qV\,(1+k)}{m_2}\right]^{1/2}} \qquad (2.9)$$

Solving for k from Equation 2.9 yields the result

$$k \leq \frac{m_2}{m_1} - 1 \qquad (2.10)$$

In other words, the energy gained through the electrical acceleration of the ions has to be larger than the "sensible" maximum initial energy by a factor of at least $1/k$ to result in resolution of the two ion peaks. Figure 2-3 presents a family of curves giving the minimum acceleration voltage as a function of $m_2$ for several assumed values of $E_o$. As in our previous example we have taken $m_1 = m_2 - 1$ meaning that an accelerating voltage greater than the value read off one of the curves at a given value of $m_2$ results in the resolution of the adjacent $m_1$ and $m_2$ ion peaks.

Of the factors considered above, those resulting in a finite pulse width at the accelerator grid (i.e. finite laser pulse length) tend to establish an upper limit to the accelerating voltage while the finite energy spread sets a lower limit to the accelerating voltage. Figure 2-4 is a composite of Figures 2-2 and 2-3 for "reasonable" values of $t_L$ = 50 ns and $E_o$ = 20 eV showing that there is a large range of accelerating voltage that provides adequate resolution of the interesting part of the atomic mass range. In the example, all of the area to the left of the shaded area would result in satisfactory resolution.

The purpose of the foregoing discussion was to provide a context for the experiments discussed in Section 3. A more comprehensive model of the ion extraction and acceleration processes that combines the various factors is described in Section 4.
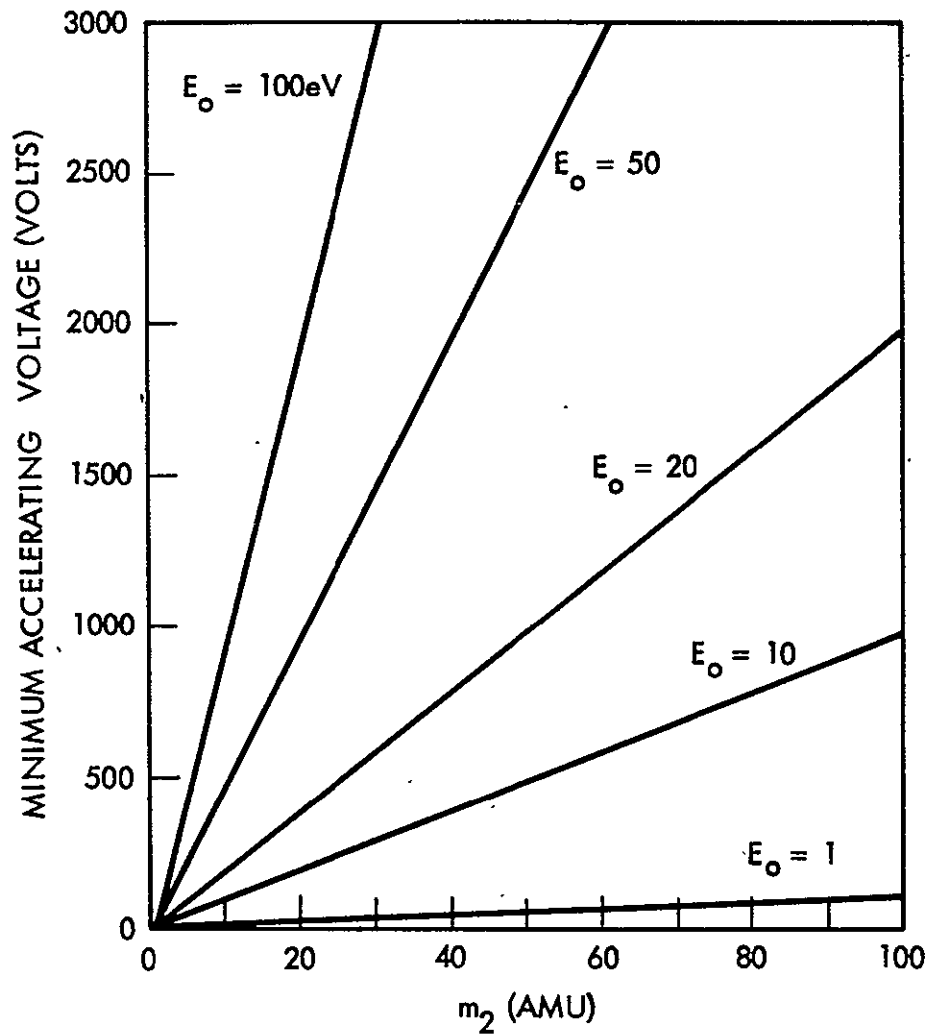
9

Figure 2-3. Minimum accelerating voltage required to give equal final velocities for ions with masses $m_2$ and $m_2-1$ for a range of initial energies of the heavier ion. The lighter ion is assumed to have zero initial energy.
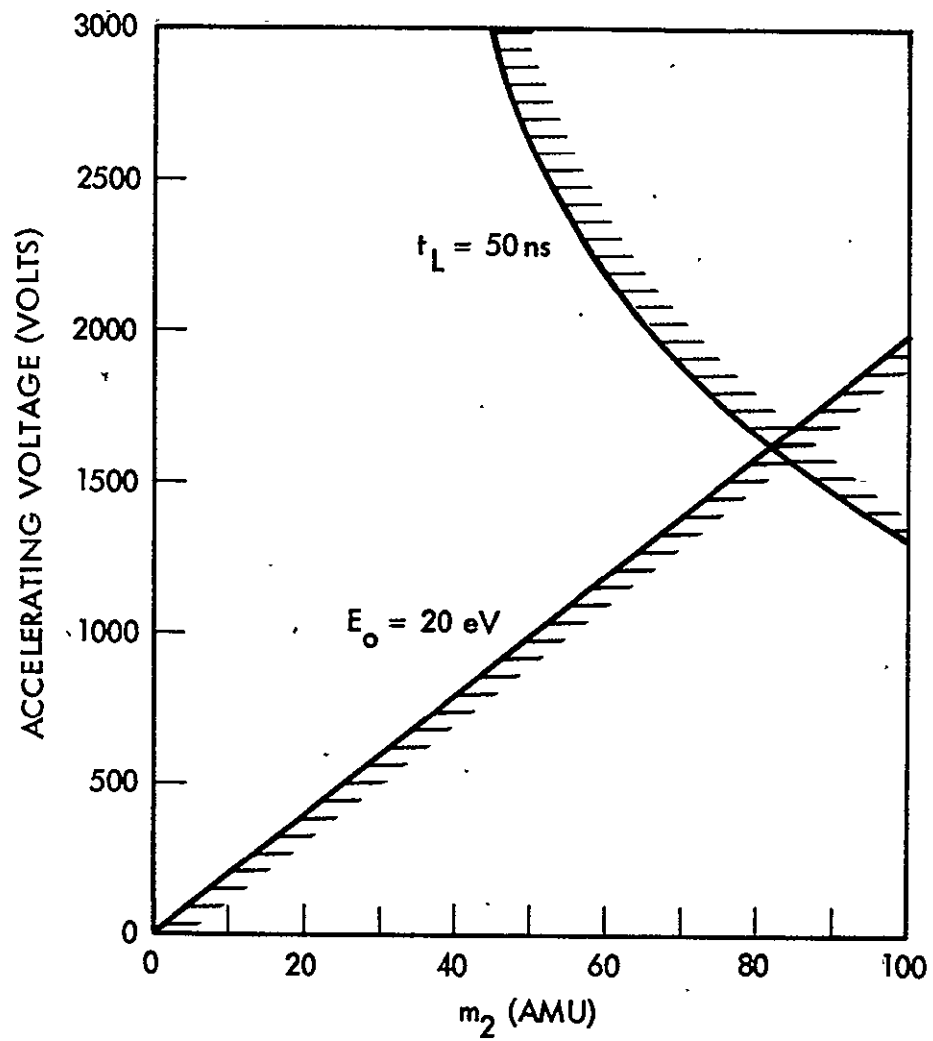
Figure 2-4.  Composite of Figures 2-3 and 2-4 that defines
the acceptable accelerating voltage range with
the two conflicting requirements.

### 2.2.2 Ionization Efficiency

When a plasma in thermal equilibrium at absolute temperature T contains several species of atoms and ions, the degree of ionization of each species $s$ whose ionization energy is $E_I{}^s$ is related to T according to Saha's equation

$$n_e n_i{}^s / n_n{}^s = CT^{3/2} U_{i,n}{}^s \exp\left(- E_I{}^s/kT\right) \qquad (2.11)$$

where $n_e$, $n_i{}^s$, and $n_n{}^s$ are the numbers per unit volume of electrons, ions of species $s$, and neutral atoms of species $s$, respectively; C is a constant; $u_{i,n}{}^s$ is the ratio $u_i{}^s/u_n{}^s$, in which $u_i{}^s$ and $u_n{}^s$ are respectively the internal partition functions of ions and neutrals of species $s$; and k is Boltzmann's constant. The Saha equation shows that the fractional ionization of a given species of atom depends on the ratio of the ionization energy of that species to the mean thermal energy of the plasma.

For a plasma containing only two atomic species, Eq. 2.11 can be written for each of the two species. Dividing one of these expressions by the other yields

$$\frac{n_i{}^{(1)}}{n_n{}^{(1)}} = \frac{n_i{}^{(2)}}{n_n{}^{(2)}} f(T) \exp\left[\left(E_I{}^{(2)} - E_I{}^{(1)}\right)/kT\right] \qquad (2.12)$$

where $f(T) = u_{i,n}{}^{(1)}/U_{i,n}{}^{(2)}$. $f(T)$ is a slowly varying function of T compared to the exponential term. Equation 2.12 shows that for nearly equal ionization potentials of the two species, the fractional ionization of the two species is nearly equal at all temperatures and the relative number of atoms of the two species can be determined by measurement of the relative number of ions. For atomic species with widely differing ionization potentials, the relative degree of ionization of the two species is strongly dependent upon T at low temperatures but the relative degrees of ionization asymptote to the same value in the limit of $kT \gg (E_I{}^{(2)} - E_i{}^{(1)})$. This argument can be readily extended to a plasma containing several atomic species.

We would not argue that the Saha equation describes the laser blow-off phenomenon because of the rapidly varying conditions within the plasma. Furthermore, Eq. 2.12 is really only valid for weakly ionized plasmas and it doesn't consider the dissociation of molecular species nor the multiple ionization of atomic species. It is fairly obvious, however, both from intuitive arguments and from the results of experiments discussed elsewhere in this report, that a high plasma temperature is required to approach comparable ionizing efficiencies for the plasma constituents. In practice, it will probably be possible to make a reasonably good estimate of the ionizing efficiency for all of the ionic species in the spectrum.

The requirement for high plasma temperature to achieve reasonably uniform ionization efficiencies results in a fairly broad initial ion energy range which, as noted above, tends to degrade the resolution of the CPA. However, the energy focus technique described in Section 4 provides a solution to this problem.

## 3. EXPERIMENTAL MEASUREMENTS

### 3.1 EXPERIMENTAL APPARATUS

The experiment consisted of three parts, the Q-switched ruby laser, the target region, and the time of flight (TOF) mass spectrometer. Each of these parts will be described in the following sections.

#### 3.1.1 Ruby Laser

The ruby laser uses a Q-switched oscillator-amplifier arrangement as shown in Figure 3-1. Both ruby rods are 10 cm long and 1.0 cm in diameter. The laser output when sampled over a central 4.4 by 7.9 mm aperture can be varied from 2.6 to 3.3 $J/cm^2$ by varying the amplifier flash lamp voltage. The laser pulse length is about 15 nsec.

For the present experiments, it was required to operate in 1-0.1 mJ energy range with a $TEM_{00}$ laser beam. An intracavity aperture-of 1 mm in diameter was used, as shown in Figure 3-1, both to reduce the laser energy as well as to give a collimated $TEM_{00}$ beam 1 mm in diameter. With a 30 cm focal length lens the laser beam is focused down to a spot of about 350 μm in diameter. This is close to the diffraction limited spot size of 300 μm.

The output energy is monitored by a beam splitter and photodiode arrangement. The beam splitter takes off about 3% of the laser energy and the photodiode is calibrated by a TRG 107 thermopile to indicate the total energy delivered to the experiment. The output energy is varied by changing the flash lamp voltage for the oscillator. For the 1-0.1 mJ energy range the laser amplifier was not usually used.

#### 3.1.2 Target Region

For the final feasibility test conducted under the present program, solid lead targets and 1:1 by atom aluminum-tin alloy targets were used. Both targets were about 2 cm in diameter and 0.3 cm thick. They were mechanically attached to a target holder which is raised to a positive voltage variable in the 0.5 to 3.0 kV range. The target holder was 7.2 cm in diameter. A grounded acceleration grid 8.9 cm in diameter

TOTAL REFLECTOR
MIRROR

POLARIZER

FLASH LAMP PUMPED
RUBY OSCILLATOR

38% OUTCOUPLER
MIRROR

BEAM SPLITTER

TO EXPERIMENT

He - Ne
ALIGNMENT
LASER

KERR CELL FOR
Q-SWITCHING

1 mm DIAMETER
APERTURE

FLASH LAMP PUMPED
RUBY AMPLIFIER
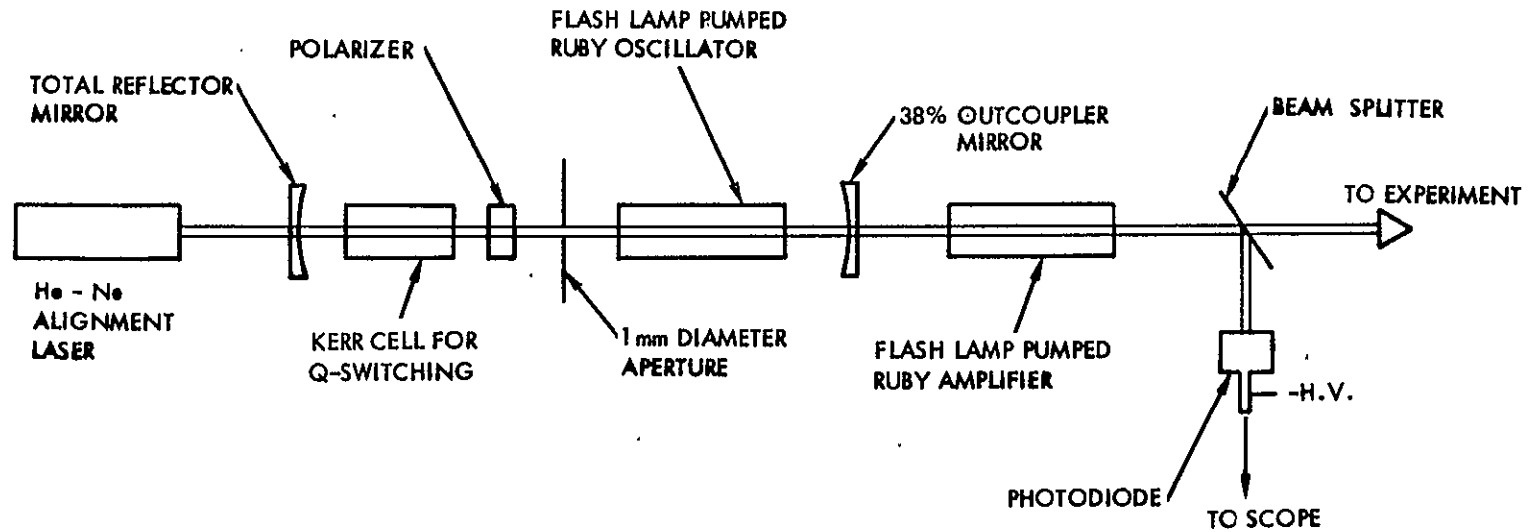
-H.V.

PHOTODIODE

TO SCOPE

Figure 3-1.  Q-Switched Ruby Laser.

is placed 2 cm in front of the target holder. This provides for extraction and acceleration of the metal positive ions formed in the laser blow off plasma.

As shown in Figure 3-2, the ruby laser beam is brought into the target region and focused down on the target by a 30 cm focal length lens. The focused laser beam is positioned on the target by two right angle total reflection prisms in a periscope arrangement. The angle of the laser beam with respect to the target normal is 27°. The focusing lens can be adjusted externally along a 7 cm travel for fine tuning of the focused spot. The spot size is approximately 350 μm in diameter. The target region and TOF mass spectrometer are maintained at $3 \times 10^{-6}$ Torr by a diffusion pump vacuum system.

### 3.1.3  Time of Flight Mass Spectrometer

The accelerated metal positive ions drift through a field free region 63 cm in length and 10 cm in diameter until they are collected on the cathode of an ion-electron multiplier. This detector is an EMI 2642-2B multiplier. A high gain current preamplifier provides the ion current verses time trace to an oscilloscope. Since the ions start traveling at the same time due to the 15 nsec laser pulse, their arrival time at the end of the drift tube is proportional to the square root of their mass to charge ratio.

For the first experiments using the lead target, the ion-electron multiplier was placed perpendicular to the drift tube axis and a six-sided grid box was used to deflect the ions into the detector. It was first thought that the initial flash of ultraviolet radiation from the laser blow-off would saturate the multiplier. The grid side facing the multiplier, designated G3, was placed at -600V and the other five sides, designated G1, were all placed at +315V. The drift region was now 110 cm, but there is about a ± 5 cm uncertainty in this length due to the actual trajectory ions follow in the deflection cage.

It was later found that the low energies used for the laser did not provide any interferring UV radiation, and the multiplier was placed end-on in the drift tube as shown in Figure 3-2 to simplify the experimental arrangement. The majority of the work done with the
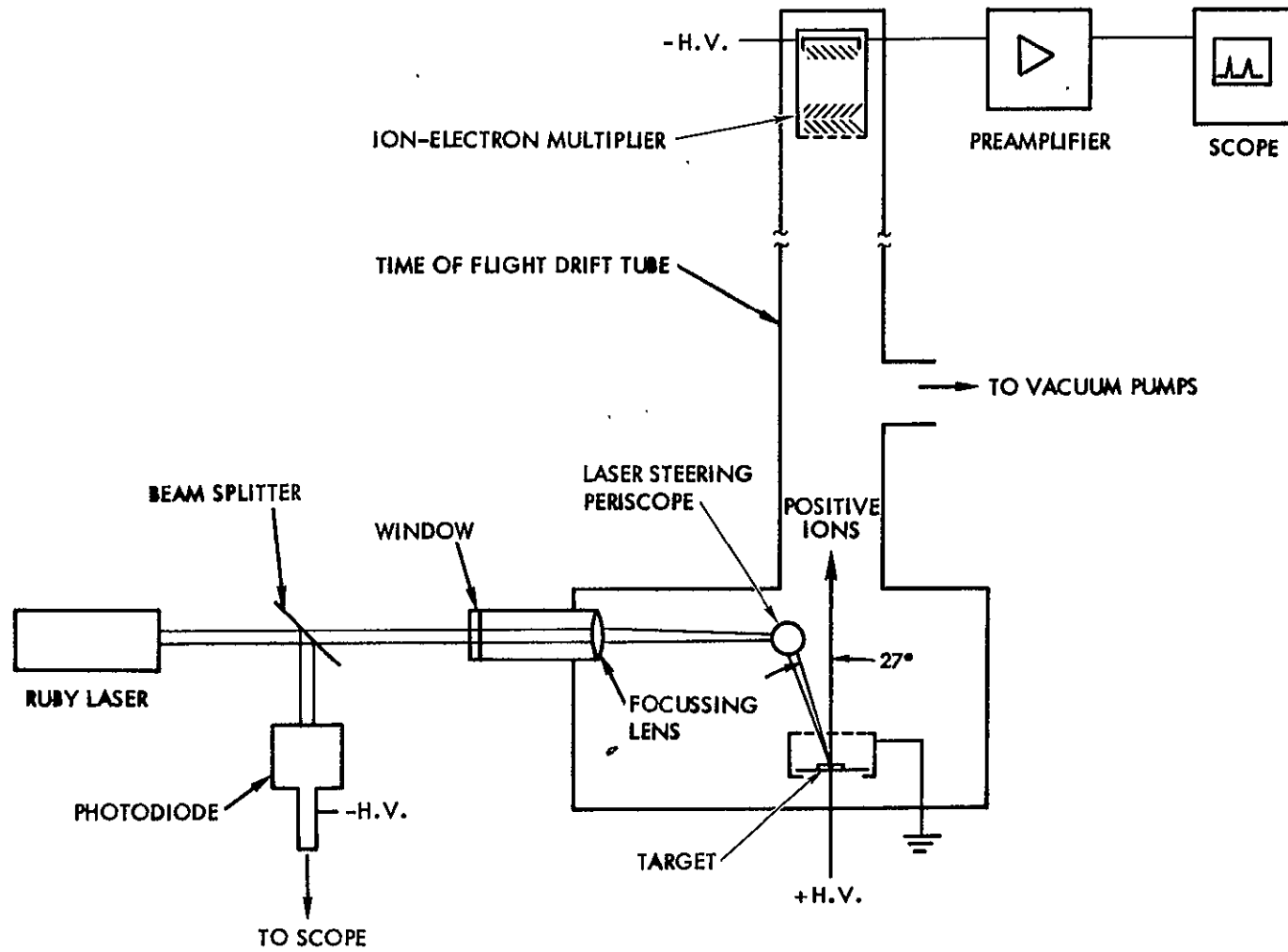
16

Figure 3-2. Experimental Apparatus.

aluminum-tin alloy target was with this configuration.

### 3.1.4 Electronic Measurements

The TOF mass spectrometer signal and the photodiode signal to monitor the energy of the laser shot were displayed an a Tektronix 7844 dual-beam oscilloscope. A high voltage probe was placed across a 0.1 μf capacitor in parallel with the acceleration voltage applied across the target grid and target holder. The output from the high voltage probe was also displayed in the oscilloscope.

When the high voltage probe is DC coupled into the scope display, the occurrence of breakdown across the acceleration gap may be monitored. At energies in excess of 0.5 mJ breakdown was usually evident caused by the dense laser blow-off plasma supplying a conductive path.

In the 0.5 -0.2 mJ energy range, breakdown was no longer a problem, but the blow-off plasma is still dense enough to result in a variety of plasma and space charge interactions. Extraction by the acceleration grid is not uniform in these instances and the TOF spectrum is very broad with distortions and false mass peaks. In these cases the high voltage probe is AC coupled and detects voltage changes of 1-10V on the several kV acceleration voltage. The voltage deflection in this range corresponds to a total ion production of $10^{12}$-$10^{13}$ ions.

Finally at laser energies of less than 0.2 mJ, well behaved TOF spectra were obtained. The high voltage probe sensitivity was limited in this range and the total number of ions produced was somewhat less than $10^{11}$ ions. This was the operating range for TOF mass spectra obtained in this program. At 0.1 mJ, the energy density corresponds to 0.1 J/cm$^2$ and power density to 7 MW/cm$^2$.

## 3.2 EXPERIMENTAL RESULTS

### 3.2.1 Major Conclusions Reached through Experiment

During the course of the experiment, it became increasingly evident that two key requirements on the laser-produced plasma bubble are critical for the success of the CPA program. These two requirements further imply a particular set of laser beam qualities, including sampled-spot size, energy, and time duration.

Requirement A: The first requirement is that the bubble temperature must be high enough for a sufficient time at the bubble atom number density produced so that a high fraction of atoms are ionized, and so that the fraction ionized depends little on species ionization potential. It appears from this present work, and from the work of others,* that this requirement can be met and that it depends on reaching a laser beam power density of $10^9$ to $10^{10}$ watts/$cm^2$ for laser pulse durations of tens of nanoseconds (and this short pulse duration is itself a requirement for the time-of-flight mass spectrometer). Unfortunately, a laser was not available to the project within the current project period which would meet Requirement A and at the same time Requirement B (to be discussed below). That is, although the required power density could be obtained, the sampled area had to be so large that too much plasma was produced for the electric accelerating field to handle. Therefore, in order that Requirement B (below) be met, power densities were limited to the order of $10^7$ W/$cm^2$. As will be discussed in detail in the next section (3.2.2), the appearance of molecular ions and disproportionately high numbers of ions from species with low ionization potentials indicates that the power density reached a barely useful level. Indeed, at somewhat lower power densities, sometimes no ions at all could be detected. On the other hand,

---

* F. Hillenkamp, E. Unsöld, R. Kaufmann and R. Nitsche, Appl. Phys. 8, 341 (1976);

R. Wechsung, F. Hillenkamp, R. Kaufmann, R. Nitsche, H. Vogt, 1979 Conference Scanning Electron Microscopy, Los Angeles, April 17-21, 1978;

J. F. Eloy, Int. J. Mass Spectrom. Ion Phys. 6, 101 (1971);

N. C. Fenner and N. R. Daly, Rev. Sci. Instr. 37, 1068 (1966).

by examining the work from the references in the preceding footnote, it appears clear that the desired results will be obtained at the $10^9$ to $10^{10}$ W/cm$^2$ level. A suitable laser is being obtained for use during the next contract phase.

Requirement B: The second key requirement is that the total amount of plasma produced be small enough so that an electric field of kilovolts/cm can separate the plasma charge in the expanding bubble in a distance of mm. It appears from the present work that this implies a production limit of less than $10^{10}$ ions per laser pulse. A great deal of time was spent in obtaining data where it was later found that the plasma bubble was large and dense enough so that part of it expanded as a neutral fluid clear across the accelerating region, and without acceleration. Under such conditions the results were extremely non-reproducible and confusing. Although it may be noted that Eloy (see preceding footnote) was able to handle above $10^{11}$ ions per shot, he also allowed the bubble to expand several centimeters before it was accelerated to 8 kV. These parameters are unacceptable for a TOF instrument; Eloy used a magnetic spectrometer with photographic plate detection. (It may also be noted that Eloy's power density was only $10^8$ W/cm$^2$, lower than Requirement A; however, his laser pulse duration was 200 nanoseconds which apparently compensated for the lower power density.)

In order to fulfill Requirements A and B at the same time, it appears necessary to limit the total laser energy to the order of $10^{-4}$ Joules for 10 nanosecond pulse durations. High total energy injected at the required temperature produces too many ions. This total energy limit coupled with Requirement A then requires a very small spot size. The projected laser beam parameters which will satisfy Requirements A and B simultaneously are given in Table 3-1.

Table 3-1. Projected Laser Beam Parameters

| | |
|---|---|
| Spot diameter | 10 to 30 x $10^{-4}$ cm (30 μm) |
| Pulse Duration | 10 x $10^{-9}$ sec |
| Total pulse energy | 0.1 x $10^{-3}$ Joules |
| ÷ Power density | $10^{10}$ to $10^9$ watts/cm$^2$ |

For the present measurements and results to be discussed in the next section, the minimum spot size obtainable with the laser and optics used was about 300 μm. If a total laser energy greater than a few tenths mJ was used, Requirement B was obviously violated and meaningless results were obtained. However, with a total laser energy of 0.1 mJ, pulse duration $10 \times 10^{-9}$ sec, and a spot diameter of 300 μm, the power density was only of order $10^7$ W/cm, thereby also violating Requirement A. The solution is, of course, to lower the total energy somewhat further and at the same time reduce the spot size to tens of micrometers. Apparatus with these capabilities is being obtained for the next contract phase.

### 3.2.2 Experimental Data

Figure 3-3 shows a series of tracings from Polaroid photographs of oscilloscope traces of ion detector current versus time. Table 3-2 lists the parameters used. Note that a constant laser spot size of 1 mm diameter was employed throughout. This spot size implies a laser energy for trace (a) of 1.1 Joules, and thus all traces were taken under conditions that grossly violated Requirement B discussed in the preceding section. However, no acceleration was present, so these traces are valid representations of the freely expanding plasma, that is, the initial plasma bubble conditions. Of particular interest in Table 3-2 is the ion energy at the distribution peak of several hundred eV, which is rising fairly slowly with power density at the higher power densities. This appears consistent with the expectation to be able to handle initial energies through energy-time focus. Also of particular interest in Table 3-2 is the rapid fall-off in number of ions produced, with power density. Actually, this is due to two effects, first, a linear decrease with total laser energy at the high power densities. This is important in meeting Requirement B as discussed in the previous section, and implies the necessity for much lower total laser energy, but with constant power density. Second, a faster fall-off sets in at lower power densities, corresponding to fewer ions produced per Joule of total laser energy and appears to be due to the lower power density. In fact, a threshold behavior occurs at even lower power density, where small random variation in total laser energy caused huge variations in total ion pulse current. However, because of Requirement A (previous section), this low power density regime is of no interest here.

100 mV/div                          20 μ sec/div    (a)

100 mV/div                          20 μ sec/div    (b)

50 mV/div                           20 μ sec/div    (c)

10 mV/div                           20 μ sec/div    (d)

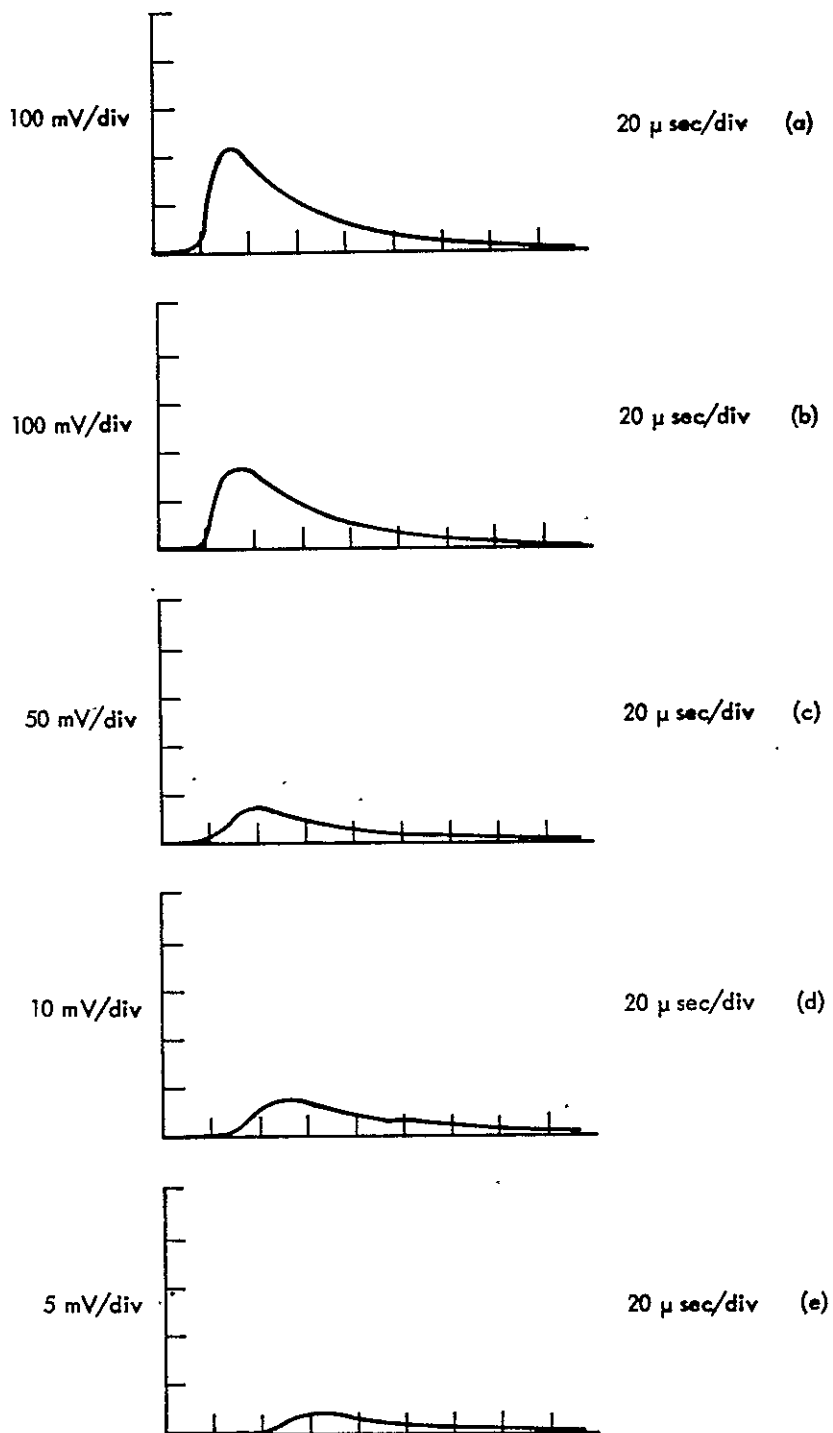5 mV/div                            20 μ sec/div    (e)

Figure 3-3.  Pulse Time Profile vs. Laser Power Density.

Table 3-2.  Ion Pulse Parameters as a Function of Laser Power Density

(Material:  Nickel; Laser:  Ruby; Laser Spot Size:  1 mm dia;
Laser Pulse:  80 nsec; Flight Length:  110 cm; Pulse Time
Profiles:  Figure 3-1)

| Profile (Fig. 3-1) | Laser Power Density (x $10^8$ W/cm$^2$) | Ion Energy at Peak (eV) | Peak Ion Current (arbitrary units) |
|---|---|---|---|
| (a) | 18 | 360 | 1.0 |
| (b) | 13 | 320 | .7 |
| (c) | 4.0 | 230 | .2 |
| (d) | 1.8 | 140 | .03 |
| (e) | 1.1 | 85 | .01 |

Figure 3-4 shows oscilloscope traces for samples of aluminum and nickel, with accelerations to 200 V and 400 V respectively, and a flight length of 110 cm, but without energy-time focus. Although Requirement B appears almost met, Requirement A is very far from being met. This can be seen from the predominance of $Na^+$ and $K^+$, which are from trace elements with very low ionization potentials. The power density here was less than $10^8$ W/cm$^2$, but the poor quality spot was not well defined. The ion peaks occur at times corresponding to essentially the acceleration energy. This implies either very little initial kinetic energy, or less than full acceleration across the accelerating region.

Figure 3-5 shows ion arrival time traces from a lead sample. Trace (a) is without acceleration and shows an initial energy at the peak (large peak) for $Pb^+$ of 200 eV. Much smaller peaks corresponding to $Na^+$ and $K^+$ still appear. Trace (b) is with 1500 V acceleration but without energy-time focus. The large peak ($Pb^+$) occurs at a time corresponding to an energy of 1200 eV, thus implying that the plasma expanded well into the accelerating region and did not gain the full acceleration. That is, both Requirements A and B were violated. A very interesting phenomenon appears in trace (b), namely that a series of ions $Pb_n^+$, with n going from 1 to at least 6 appears to be produced under the laser bombardment conditions obtaining here. The power density was between $10^7$ and $10^8$ W/cm$^2$, but the laser spot was $TEM_{00}$ as contrasted to Figure 3-4 in which a multimode spot was used. Hence, a direct comparison of power density is difficult.

Figure 3-6 shows traces from a sample of 50-50 tin-aluminum alloy. The flight length was 63 cm, and no energy-time focus was used. Again Requirements A and B are violated. Thus, at the insufficient power density obtaining for trace (a), a series of molecular ions is observed. The power density for trace (b) was somewhat higher, but this caused a greater violation of Requirement B, while improving on Requirement A. In this case roughly equal amounts of the major species were observed, with much fewer molecular ions.

10 μ sec/div

(a)

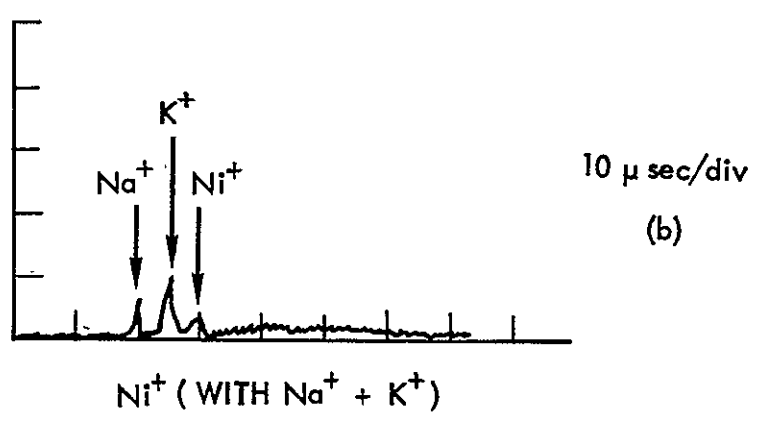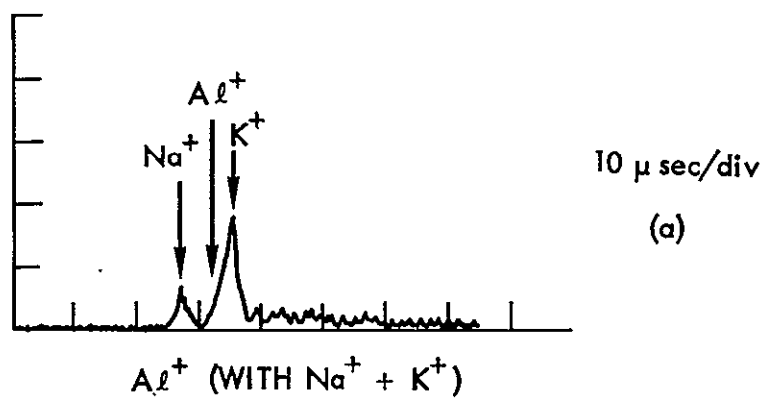Aℓ⁺ (WITH Na⁺ + K⁺)

10 μ sec/div

(b)

Ni⁺ ( WITH Na⁺ + K⁺ )

Figure 3-4.  Aluminum and Nickel Targets at Very Low Power Density.

20 μ sec/div

(a)

Pb$^+$ (WITH Na$^+$ AND K$^+$)
NO ACCELERATION

20 μ sec/div

(b)
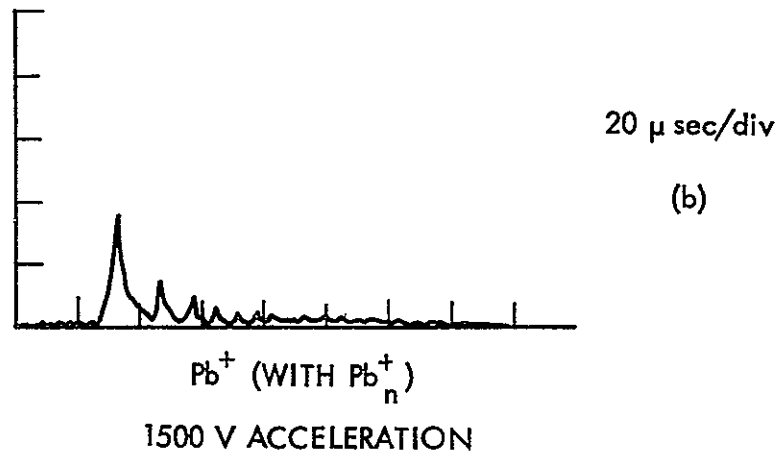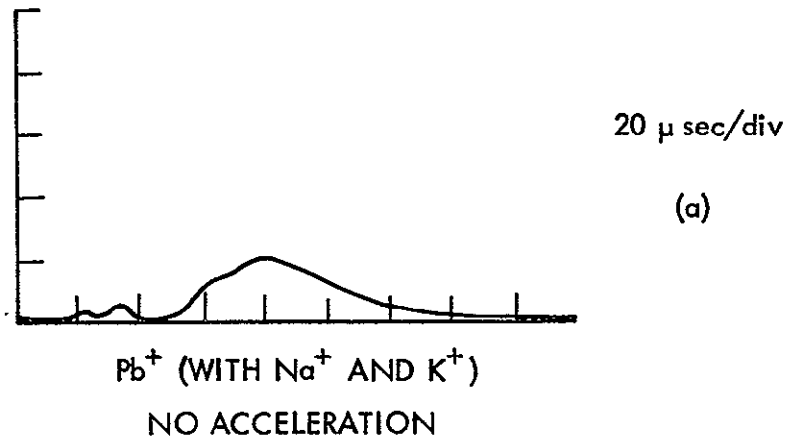
Pb$^+$ (WITH Pb$_n^+$)
1500 V ACCELERATION

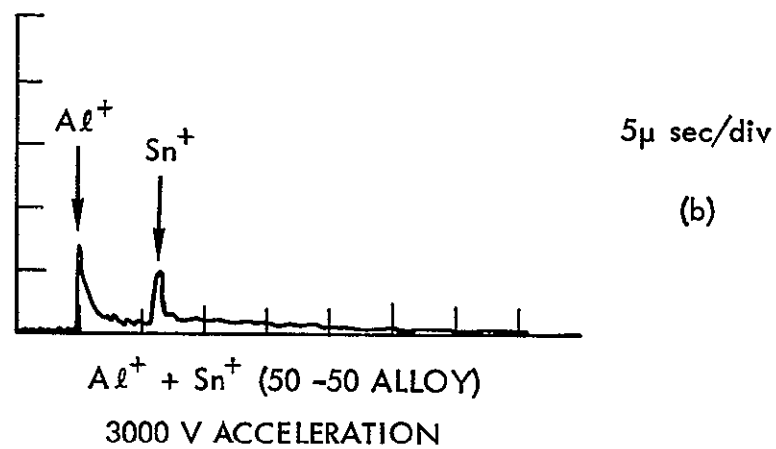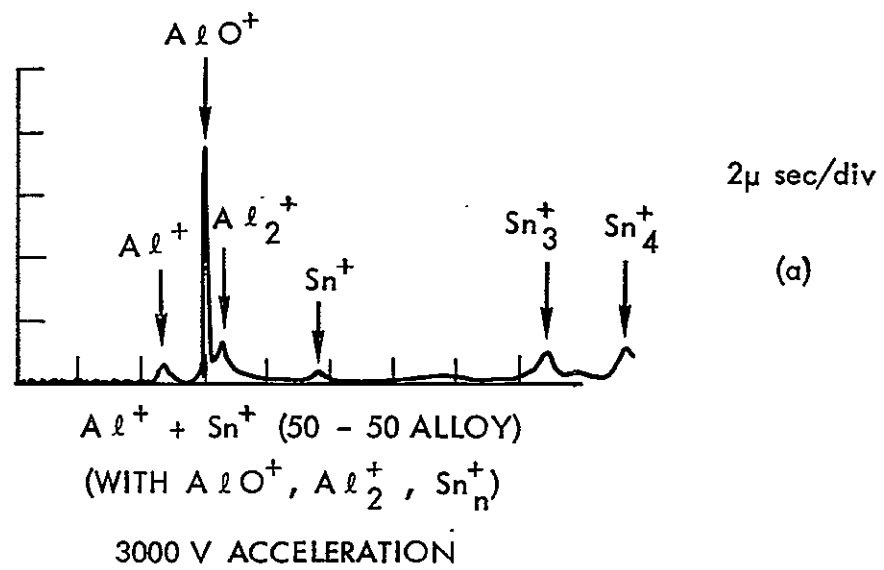Figure 3-5.  Lead Target at Low Power Density.

Figure 3-6. Tin and Aluminum Alloy Target at Low Power Density.

## 4. ENERGY-TIME FOCUS FOR TIME OF FLIGHT MASS SPECTROMETERS

### 4.1 INTRODUCTION

A time-of-flight (TOF) mass spectrometer operates on the principle that particles with the same kinetic energy but with differing masses have different speeds and, therefore, traverse the same path between two points with different "flight times." By measuring the particle arrival times it is possible to associate the arrival times with the particle mass and thereby determine the "mass spectrum" of particles passing through the TOF instrument. In order that the arrival times for all particles of a given mass be identical, it is necessary that they all start their "flight" at the same time with the same kinetic energy. In any practical instrument there always exists a spread in both starting time and energy, and the amount of spread determines the "mass resolution." That is, if the spread in starting times for particles of two masses is greater than the difference in their flight times, their arrival time peaks will overlap and they will not be resolved. Initial energy spread has a similar effect by also broadening the arrival-time peaks for individual masses.

The energy-time focus device described here reduces drastically the effect of initial energy spread by adding additional flight-time to all particles (ions), with more being added to the initially faster ions which would otherwise arrive "too early." That is, the normal flight-time plus the added time in the device sums to a total time which is largely independent of the initial energy. Therefore, all ions of a given mass, but with a spread in initial energy, arrive at almost the same time at the detector, and at a time different from other masses. This constitutes essentially an "energy-time focus."

The active element of the device consists of a uniform electric field placed at the end of the normal flight tube of a TOF mass spectrometer. The field strength and direction are adjusted so that the ions are stopped and reflected almost back on their original path in a distance one-fourth the length of the normal flight path. (This assumes a negligible time spent in the first acceleration region, and that the energy due to the first electric acceleration is much greater than the initial

energy spread. The value "one-fourth" may be adjusted slightly to compensate for partial failure of these assumptions.)

Figure 4-1 shows a schematic drawing. A usual TOF mass spectrometer has the detector entrance at the same location, but pointed toward the ion source. The "reflection region" constitutes the device to be described here. It could be appended to any TOF ion spectrometer in which initial energy spread is troublesome, in order to increase mass resolution. The uniform electric field is produced within a series of "guard rings" held at potentials appropriate to produce the necessary uniform electric field. The reflection region is terminated by screens or plates at the ends.
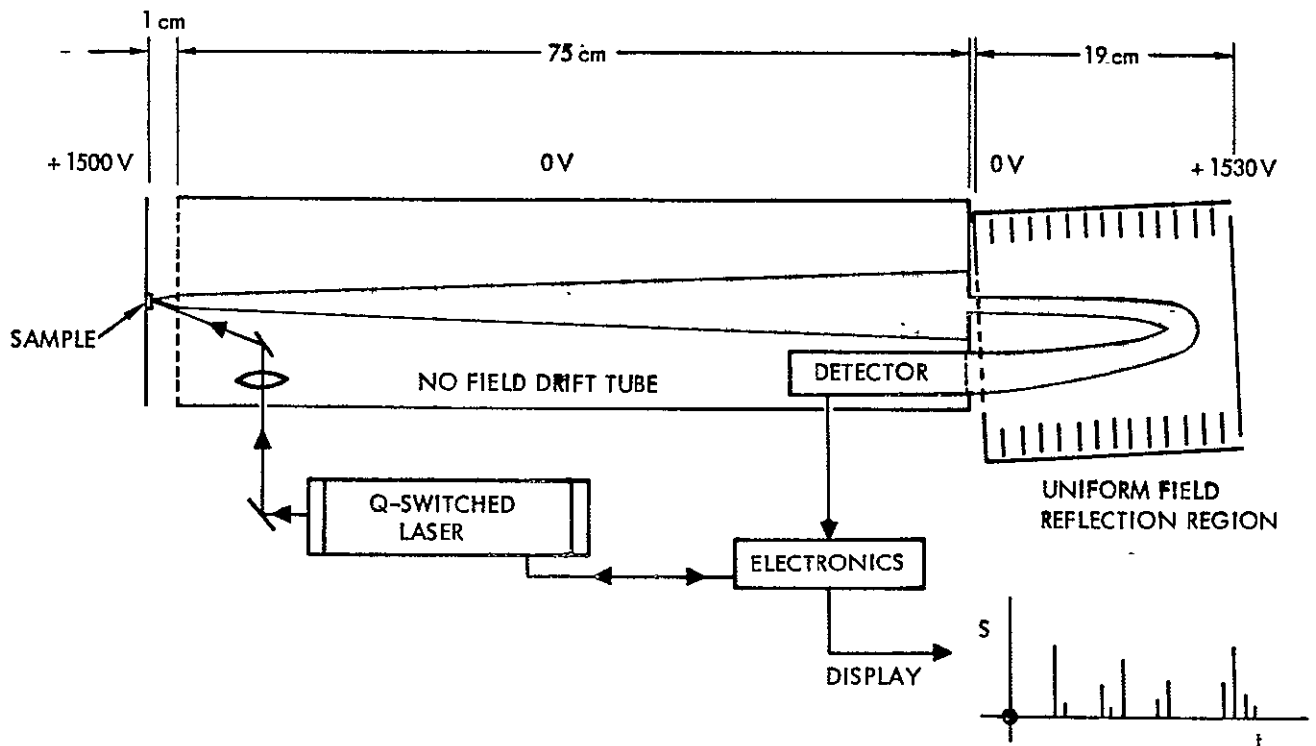
Figure 4-1. Schematic Diagram of TOF Mass Spectrometer with Laser Blow-Off Ion Source and Energy-Time Focus.

29

## 4.2 THEORY OF ENERGY-TIME FOCUS

In a usual time-of-flight (TOF) mass spectrometer, ions of a given mass will arrive at the detector at precisely the same time only if they travel the same free flight distance after starting at precisely the same time with precisely the same initial kinetic energy. In any practical TOF instrument neither the starting times nor the starting kinetic energies are precisely equal for all ions of even the same mass. Thus, for a free-flight path of length L meters for ions of mass in kilograms with charge q Coulombs accelerated across a potential difference V volts and having initial kinetic energy $E_0$ Joules, the free-flight time t seconds is given by

$$t = L \cdot \left[2(qV + E_0)/m\right]^{-1/2} \quad . \tag{4.1}$$

Now if all the ions have zero initial energy, the difference in arrival times $\Delta t_m$ for two masses m and m + $\Delta$m is approximately given by

$$\Delta t_m \approx \frac{dt}{dm} \cdot \Delta m = \frac{d}{dm}\left(\frac{L}{\sqrt{2qV}} m^{1/2}\right) \cdot \Delta m = \left(\frac{Lm}{2\sqrt{2qV}}^{-1/2}\right) \cdot \Delta m \quad . \tag{4.2}$$

This $\Delta t$ represents the time between the signal "spikes" for masses m and m + $\Delta$m. Clearly if the ions of mass m (and/or mass m + $\Delta$m) have starting time spreads greater than or about equal to $\Delta t_m$, or if the electronic circuitry cannot resolve signal peaks occurring within $\Delta t_m$, then masses m and m + $\Delta$m will not be resolved by a TOF mass spectrometer with parameter values determining $\Delta t_m$ through Eq. 4.2. For example, in order to resolve a particular mass m from mass m + $\Delta$m, it might be necessary to increase L or reduce V. These considerations are extremely important to the over-all conclusion of this report, but it will be assumed for the present discussion that $\Delta t_m$ for masses m and m + $\Delta$m of interest is large compared to starting time spread and electronic detection time resolution. Under this assumption, resolution will be limited by the spreads in initial ion kinetic energy $E_0$, as seen from Eq. 4.1. The arrival time difference $\Delta t_{E_0}$ for two ions of mass m, but having initial energy $E_0 = E_0$ and $E_0 = 0$ is given by

$$\Delta t_{E_0} = L \cdot \sqrt{\frac{m}{2}} \cdot \left\{ (qV)^{-1/2} - (qV + E_0)^{-1/2} \right\}$$

$$= \frac{Lm^{1/2}}{\sqrt{2qV}} \cdot \left\{ \frac{E_0}{2qV} + \cdots \right\} \tag{4.3}$$

When the spread in $E_0$ becomes sufficiently large, that is, when $\Delta t_{E_0}$ is larger than or about equal to $\Delta t_m$ for two masses m and $\Delta m$ of interest, then m and m + $\Delta m$ cannot be resolved. It may be noted that increasing L does not help in this case since both $\Delta t_m$ and $\Delta t_{E_0}$ increase linearly with L. Increasing the acceleration voltage V does reduce the effect of $E_0$, but at the cost of decreasing $\Delta t_m$ for a given m and m + $\Delta m$ which is eventually limited by starting time spread and electronic detection time resolution as discussed above in this section.

By equating $\Delta t_m$ and $\Delta t_{E_0}$ from Eqs. 4.2 and 4.3 and taking $\Delta m = 1$, the following approximate expression is found.

$$m \cong qV/E_0 \tag{4.4}$$

This implies that the mass number m which can barely be resolved from the adjacent mass number because of mass m having a spread in initial kinetic energy $E_0$ is given by the acceleration energy divided by the initial energy spread $E_0$. For the actual TOF spectrometer configuration being considered here, $E_0$ may easily be as high as 50 eV, while length L and starting time considerations limit qV to 1500 eV. Thus, masses higher than mass 30 would not be resolved. Clearly this is unacceptable, and in order to solve this problem, the following energy-time focus technique was discovered.

The desired result is that two ions of mass m but having differing initial energy $E_0 = 0$ and $E_0 = E_0$ arrive at the detector at the same time, that is, that the flight time not depend on $E_0$. It is seen from Eq. 4.1 that this is not the case for a simple free-flight TOF spectrometer. However, by adding a "reflection region" to the total flight path in which the ions slow to a stop and are reflected back to the detector, it is possible to produce a total travel time which is independent of initial energy to second order in $E_0/qV$, and for which this "focus"

31

condition does not depend on m. Consider the time trajectory of an ion entering a uniform electric field, $\vec{\epsilon}$, whose direction is opposite to the velocity $v_0$ of the ion when it enters the uniform field region. Let x, v, and a represent the distance traveled in the direction against the field, the speed along x, and the acceleration along x, respectively. $-\vec{\epsilon}$ is also along x, so the problem is one dimensional, and

$$a = \frac{-q\epsilon}{m} \qquad\qquad (4.5a)$$

$$v = \frac{-q\epsilon}{m} t + v_0 \qquad\qquad (4.5b)$$

$$x = \frac{-q\epsilon}{2m} t^2 + v_0 t \qquad . \qquad (4.5c)$$

The time to reflect back to the starting (entry) point, $t_r$, is twice the time to stop, $t_s$, which is given from Eq. 4.5b as

$$t_r = 2 \cdot t_s = 2 \cdot \frac{v_0 m}{q\epsilon} = \frac{2m}{q\epsilon}\left[\frac{2}{m}(qV + E_0)\right]^{1/2} \qquad . \qquad (4.6)$$

The total flight time $t_T$ for an ion is then the free flight time given by Eq. 4.1 plus the reflection time $t_r$ given by Eq. 4.6.

$$t_T = L \cdot \sqrt{\frac{m}{2}} \cdot (qV + E_0)^{-1/2} + \frac{2m}{q\epsilon}\sqrt{\frac{2}{m}} (qV + E_0)^{1/2} \qquad . \qquad (4.7)$$

Now if one makes the stopping field $\epsilon$

$$\epsilon = 4 \cdot V/L \qquad , \qquad\qquad (4.8)$$

one obtains the result

$$t_T = L \cdot \sqrt{\frac{m}{2}} \cdot \frac{1}{\sqrt{qV}} \cdot \left\{(1 + E_0/qV)^{-1/2} + (1 + E_0/qV)^{1/2}\right\} \qquad (4.9)$$

and expanding,

$$t_T = L \cdot \sqrt{\frac{m}{2}} \cdot \frac{1}{\sqrt{qV}} \cdot \left\{1 - \frac{E_0}{2qV} + \frac{3E_0^2}{8q^2V^2} - \ldots + 1 + \frac{E_0}{2qV} - \frac{E_0^2}{8q^2V^2} + \ldots\right\}$$

$$= 2 \cdot L \cdot \sqrt{\frac{m}{2}} \cdot \frac{1}{\sqrt{qV}} \cdot \left\{1 + \frac{1}{8}\left(\frac{E_0}{qV}\right)^2 - \ldots\right\} \qquad . \qquad (4.10)$$

Upon inspection of Eq. 4.10 it may be seen that the total flight time $t_T$ is, to first order, just twice the normal TOF flight time without a reflection region for an ion with $E_0 = 0$, as given in Eq. 4.1; furthermore, the first order terms in $E_0/qV$ cancel out along with a fraction of the second order terms. For this case the $\Delta t_{T,m}$ time difference between arrival of masses m and m + $\Delta$m is twice $\Delta t_m$ from Eq. 4.2,

$$\Delta t_{T,m} \cong \left( \frac{L m^{-1/2}}{\sqrt{2qV}} \right) \cdot \Delta m \tag{4.11}$$

and in analogy to Eq. 4.3 for two particles of mass m but with $E_0 = 0$ and $E_0 = E_0$, the $\Delta t_{T,E_0}$ is given by

$$\Delta t_{T,E_0} \cong - 2 \cdot L \cdot \sqrt{\frac{m}{2qV}} \cdot \frac{1}{8} \left( \frac{E_0}{qV} \right)^2 \tag{4.12}$$

Again in analogy to obtaining Eq. 4.4, if $\Delta t_{T,m}$ and $\Delta t_{T, E_0}$ in Eqs. 4.11 and 4.12 are set equal and $\Delta$m = 1, one obtains

$$m \cong 4 \left( \frac{qV}{E_0} \right)^2 \tag{4.13}$$

This implies that the mass number m which can barely be resolved from the adjacent mass number because of m having an initial energy spread $E_0$ is not reached until mass 3600 for an acceleration to 1500 eV with $E_0 = 50$ eV. This is contrasted to a limit of mass 30 for the same TOF conditions without the energy-time focus reflection region, as discussed with Eq. 4.4. It is not likely that a resolution of 3600 will be reached here because of starting time spread and three-dimensional effects in the reflecting region, since the ions must be reflected at a slight angle in order to reach a detector outside the original ion path before reflection.

Equation 4.8 states the condition on the reflecting $\varepsilon$ field magnitude which must be satisfied to obtain energy-time focus. Consider first an ion with $E_0 = 0$. It must reach a potential equal to V at the time it stops and reverses, and the distance X it traverses to that point must satisfy

$$\varepsilon \cdot X = V , \tag{4.14}$$

but Eq. 4.8 requires that $\epsilon = 4 \cdot V/L$.  Hence

$$X = L/4 \quad , \tag{4.15}$$

is the necessary condition on X.  That is, the field must be uniform and such that an ion with $E_0 = 0$ stops and reflects at a distance into the reflection region of L/4, where L is the normal TOF flight path without energy-time focus.

The reflection region must be long enough to accommodate ions with initial energy $E_0 > 0$.  However, it is possible to utilize an end plate on the reflection region to remove particularly high energy ions from the "tail" of the initial energy distribution, thereby providing a low pass energy filter to limit the energy spread $E_0$.

The theoretical value "4" required by Eq. 4.8 is correct for the ideal case where all ions start at the same time into the free-flight region, and are reflected exactly back along their original paths in the reflection region.  It is likely that for a practical instrument, where ions are first accelerated over a finite region before entering the free-flight region and are reflected at a slight angle to the detector and where some space charge effects may become significant, the best number may not be "4".  Indeed, the computer simulation to be described next indicated that "3.8" was a better value for the specific parameters used.  This is easily varied in practice by varying the potential across the length of the reflection region to "tune" the focus.

4.3 COMPUTER SIMULATION OF TOF SPECTROMETER WITH ENERGY-TIME FOCUS

As a major part of the program to show feasibility for a laser blow-off time-of-flight mass spectrometer for cometary particulate analysis, a one-dimensional Monte Carlo computer simulation was developed.  The computer simulation program evolved over the course of the project as new approaches and techniques were added or discarded.  It became evident very early that the spread in ion initial kinetic energy of 10's to 100's of eV presented a severe problem if mass resolution of 100 was to be obtained while maintaining an overall length less than one meter.

This evolution eventually led to the energy-time focus technique discussed above in Section 4.2, which appears to have solved the problem

of initial ion energy. Although the earlier ideas and attempts were unsuccessful, they will be discussed briefly in the interests of complete documentation.

All versions of the computer simulation have included a Monte Carlo random choice for each ion of starting time after zero, initial position in the first acceleration region, and initial kinetic energy. Starting time distributions were represented by the same function as the charge and discharge of a simple RC electrical network, with an exponential rise followed by an exponential decay back to zero. The RC time-constant and the number of time constants for "on" could be chosen. Thus, an RC of one nanosecond, "on" for 30 time constants produces an almost uniform distribution lasting 30 nanoseconds; a peaked distribution results from "on" of a few time constants. This distribution was originally picked to simulate ions produced by a pulsed electron beam, for which the distribution is a good representation. It is adequate to show "worst case" simulation for the laser produced plasma under the assumption that ions are only produced during the laser pulse. Implicit in this assumption is negligible "extraction time" for ions from the plasma bubble by the electric field; actually the bubble must expand to some degree before the ions "start". This part of the simulation becomes more accurate as the total number of ions produced decreases to the point where plasma bubble effects are negligible.

The distribution of initial ion positions is represented by a normalized polynomial $(1 + ax + bx^2 + cx^3)$ for x in centimeters. If the polynomial becomes negative, the distribution is taken as zero from that point on. For example, if b is -400 then the distribution falls from maximum at $x = 0$ quadratically to zero at $x = 0.05$ cm. Again, this distribution was originally used to represent the distribution of electrons in a pulsed ionizing electron beam, which determined the ion initial position distribution. In the case of the laser blow-off-produced plasma bubble, this distribution can be used to determine an estimate of the "worst case" effect for a given initial position distribution in the accelerating field. However, since the plasma is conducting to some point in its expansion, the actual spread in final ion energy will be less than in the absence of plasma. This distribution leads to a "worst case" so

long as all ions are extracted from the plasma within the region represented by the chosen distribution function parameters. This part of the simulation also increases in accuracy as the total number of ions produced decreases to where plasma bubble effects are unimportant.

The distribution function for initial ion energies (velocities) was taken as a one-dimensional Maxwellian distribution given by

$$dN_x = N \left(\frac{m}{2\pi kT}\right)^{1/2} \exp\left(- mv_x^2/2kT\right) dv_x \quad , \quad (4.16)$$

where N is the total number of ions, m is ion mass, $v_x$ the speed, and kT the Boltzmann energy (temperature). This distribution function is expected to be a good representation of the initial energy of the ions from a freely expanding laser blow-off-produced plasma bubble. Actually, it has been noted earlier* that the plasma particle velocities are best represented by a lower thermal temperature coupled to a "blow-off velocity" of the center-of-mass of the bubble. However, the velocity distribution along the normal to the source plane producing the bubble is well represented by assuming a higher temperature (kT) and ignoring the "blow-off velocity." The computer simulation is able to handle a separate "blow-off velocity" parameter, but the facility was not used. In the cases where the plasma bubble does not expand freely, but expands within a strong electric field, the degree of validity is uncertain. However, comparison with results of reported measurements[†] indicates that use of kT = 200 eV produces an initial energy distribution for simulation as broad as or broader than those measured under similar electric field conditions.

With the starting time, position, and initial energy of each ion chosen by random numbers (Monte Carlo), simulations of time-of-flight (TOF) mass spectrometers were made for a number of TOF configurations.

---

*N. G. Utterback, S. P. Tang, and J. F. Friichtenicht, Phys. Fluids 19, 900 (1976).

†J. F. Eloy, Int. J. Mass Spectrom. Ion. Phys. 6, 101 (1971); E. Hillenkamp, E. Unsold, R. Kaufmann and R. Nitsche, Applied Phys. 8, 341 (1975); N. C. Fenner and N. R. Daly, Rev. Sci. Instr. 37, 1068 (1966).

The simplest consisted of an acceleration region in a uniform electric field followed by a field-free flight region. Figure 4.2 shows the simulated mass (time) spectrum obtained for this configuration for the parameters and Monte Carlo distributions given in Table 4-1, for the example spectrum of masses given in Table 4-2. It is immediately clear from Figure 4-2 that this simple TOF instrument configuration with a laser blow-off ion source is unacceptable if a mass resolution of 100 is to be obtained. Even if the initial energy distribution is determined by kT = 20 eV rather than 200 eV, the same result obtains. For this reason a number of attempts were made via simulations of other techniques and configurations to solve this problem of high initial kinetic energy.

The first attempt involved a time delay after the laser pulse in turning on the accelerating field. This allowed the ions to distribute themselves spatially within the accelerating region according to their initial energy before the accelerating field was established; thus a "faster" ion would have moved further across the acceleration region before the field was applied and would therefore receive less energy from the accelerating field. The initially "slower" ion would then catch up to the initially "faster" ion just at the detector, producing a focus in time for ions of differing initial energy. This scheme does produce a reasonable time focus for a small mass number range for a given delay setting, but the delay setting must be changed for each mass number region to be studied. Furthermore, the focus is not sufficiently independent of initial ion energy to produce fully acceptable results.

A second attempt again involved a pulsed accelerating field, but rather than being turned on and left on after a delay time, the field was turned on and then off before ions reached the end of the accelerating region. This acceleration produced an equal "impulse" for all ions, resulting in mass separation in arrival times varying directly as m rather than $\sqrt{m}$ as with the other techniques. However, the initial energy spread was still sufficient to cause arrival time overlap and unacceptably low mass resolution. Also prohibitively high accelerating potentials and slew rates would be necessary.

A third technique was attempted which involved an energy selector which allowed only a narrow energy spread of ions to pass to the detector,
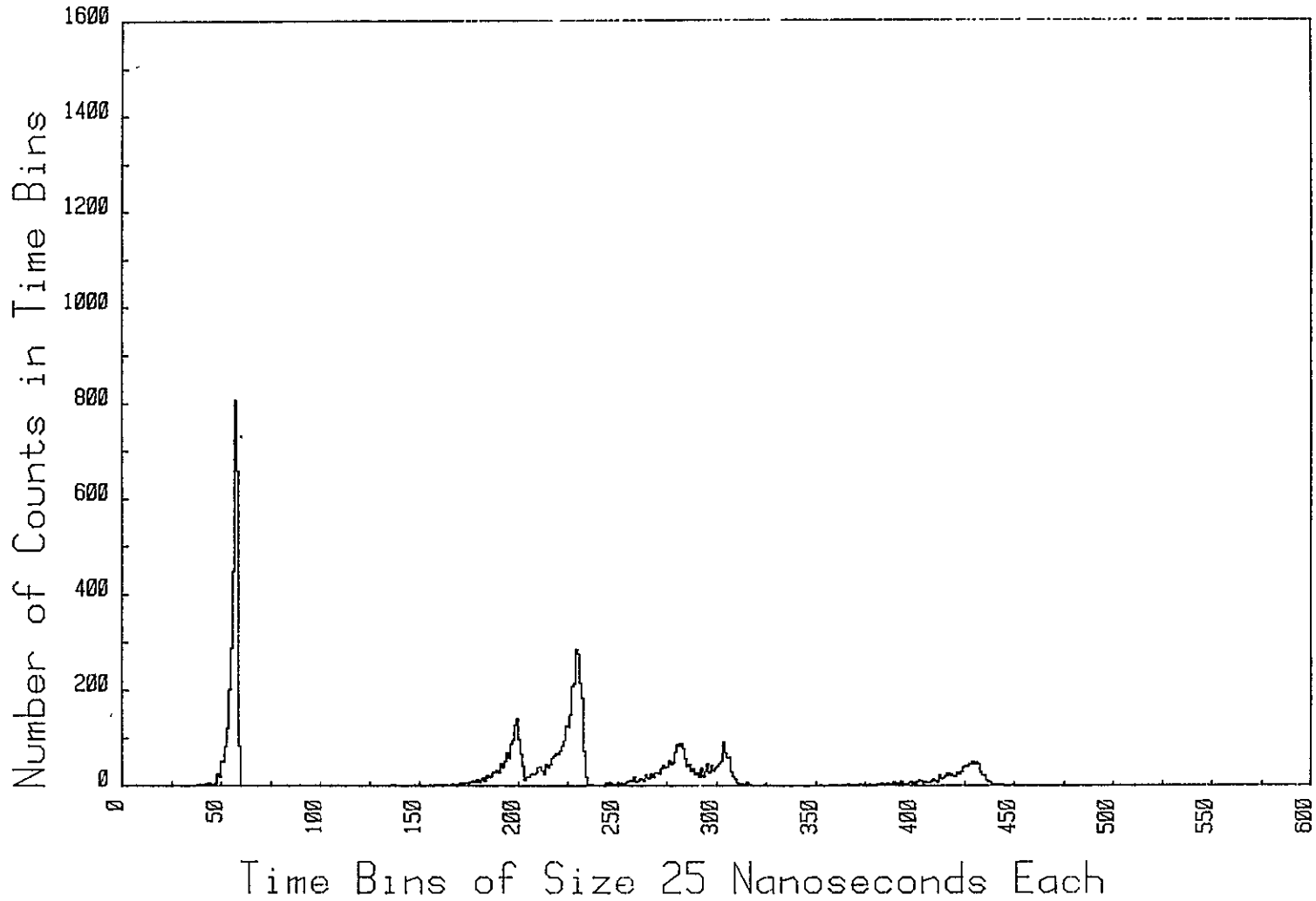
Figure 4-2.  Mass Spectrum Without Energy-Time Focus.

Table 4-1.  TOF Simulation Parameters and Initial Distribut
(Figure 4-2)

| | |
|---|---|
| Length of Acceleration Region | 1 cm |
| Length of Field-free Flight Region | 75 cm |
| Acceleration Energy | 1500 eV |
| TOF Arrival Time Bin Size | 25 ns |
| Number of Particles Injected | 10,000 ions |
| Starting Time Distribution: | |
| Uniform over first | 30 ns |
| Starting Position in Accelerating Region: | |
| Quadratic fall-off from maximum to zero in first | 0.5 mm |
| Starting Kinetic Energy Distribution: | |
| Maxwellian with kT equal to | 200 eV |

and, in addition, for the case with Energy-Time Focus
(Figures 4-3 and 4-4)

| | |
|---|---|
| Length of Reflection Region | $\sim$ 20 cm |
| Reflection Parameter: (simple theoretical value 4) | 3.8 |
| Upper Energy Limit: (defined by physical end of reflection region) | 1530 eV |

Table 4-2. Number Distributions of Masses
for Computer Simulations

| SPECIES | MASS | ATOM FRACTION (%) |
|---------|------|-------------------|
| H | 1 | 28.7 |
| C | 12 | 11.4 |
| C | 13 | 0.1 |
| 0 | 16 | 28.6 |
| 0 | 18 | 0.1 |
| Mg | 24 | 9.0 |
| Mg | 25 | 1.2 |
| Mg | 26 | 1.3 |
| Si | 28 | 8.8 |
| Si | 29 | 0.4 |
| Si | 30 | 0.3 |
| Fe | 54 | 0.6 |
| Fe | 56 | 8.9 |
| Fe | 57 | 0.2 |
| Ni | 58 | 0.3 |
| Ni | 60 | 0.1 |

thus throwing out ions with widely divergent energy and, therefore, having potential arrival time overlap. This technique required an energy selector with unacceptably high energy resolution and low transmission.[†]

Finally, the Energy-Time Focus technique utilizing a reflection region, and described in detail in Sections 4.1 and 4.2, was discovered. It appears to be the solution to the problem of the high initial energy spread. Figures 4-3 and 4-4 show the results with Energy-Time Focus using the same parameters for the TOF simulation as Figure 4-2 (Tables 4-1 and 4-2), but with the added reflection region.

A direct comparison of Figure 4-2 with Figures 4-3 and 4-4 shows the great improvement in mass resolution resulting from Energy-Time Focus with a reflection region.

---

†It was later discovered that this technique has been previously used, and was limited to a mass resolution of 30. See N. C. Fenner and N. R. Daly, Rev. Sci. Inst. 37, 1068 (1966).
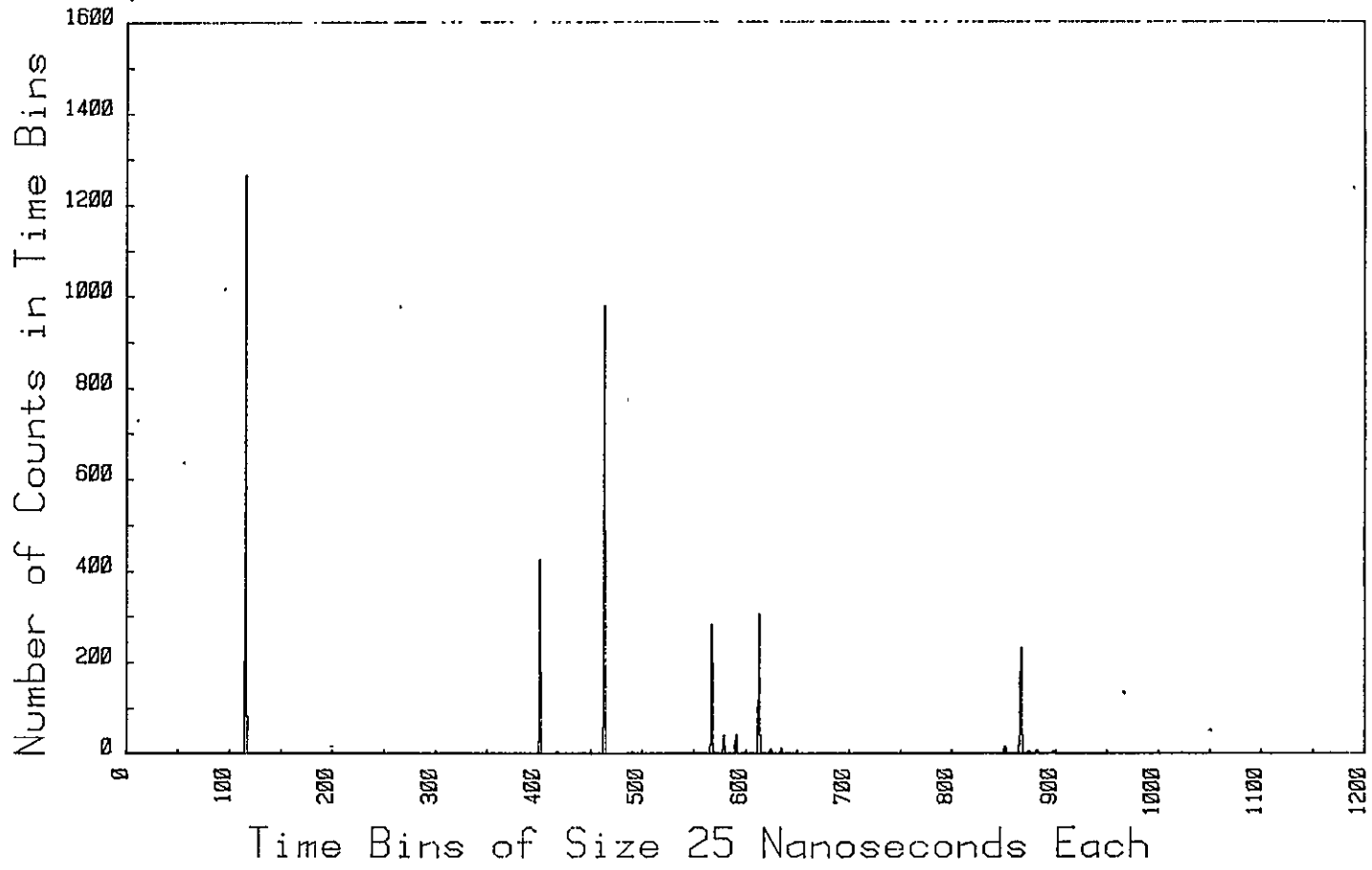
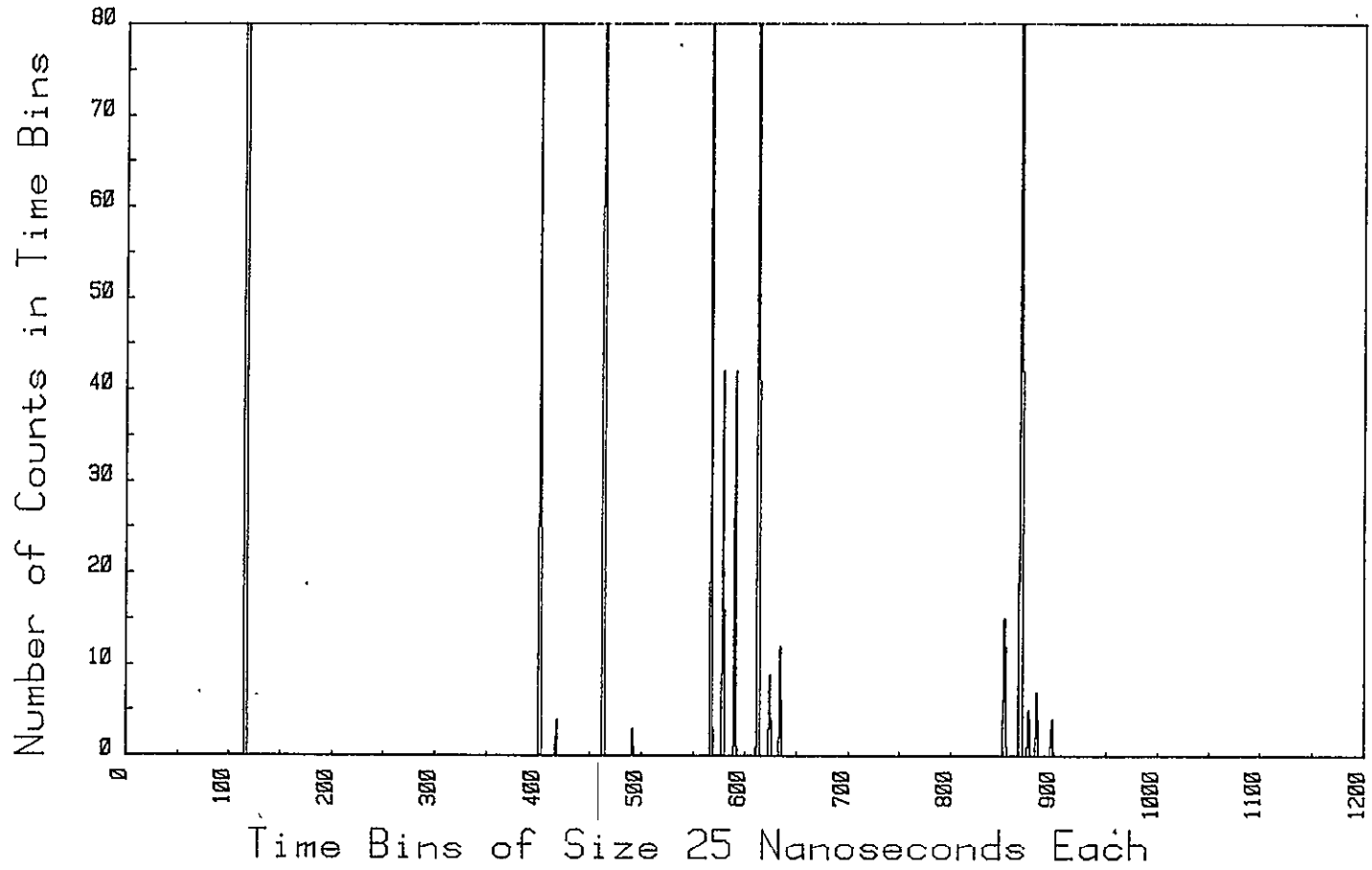Figure 4-3. Mass Spectrum with Energy-Time Focus (Low Sensitivity).

Figure 4-4.  Mass Spectrum with Energy-Time Focus (High Sensitivity).

## 5.  BASELINE INSTRUMENT SPECIFICATIONS

On the basis of the efforts conducted under this program, some of the parameters of the CPA have undergone significant modification from our original estimates.  Here, we will simply summarize in tabular form the new numerical values of some of these parameters.

### Laser System

| | |
|---|---|
| Laser pulse energy: | 0.1 to 1.0 mJ |
| Pulse duration: | $\sim$ 10 ns |
| Spot size at collector: | 10 to 100 $\mu$m diameter |
| Power density at collector: | $10^9$ to $10^{10}$ watts cm$^{-2}$ |
| Pulse repetition rate: | TBD |
| Laser wavelength: | UV, visible, near I-R |

### TOF Range (with Energy Focus)

| | |
|---|---|
| Collector to grid spacing, $L_1$: | 1 to 3 cm |
| Ion drift region length, $L_2$: | 75 cm |
| Ion reflection region length: | $L_2/4$ |
| System diameter: | TBD |
| Accelerating voltage: | 5000 to 1500 V |
| Decelerating voltage: | 3500 to 0 V |

### Electronics

| | |
|---|---|
| Ion Detector: | Electron multiplier/channeltron |
| Ion detector sensitivity: | TBD |
| Ion detector dynamic range: | TBD |
| A/D conversion rate: | 50 nsec |

# 6. SUMMARY

At the beginning of this program we believed that our major objective was to find those laser bombardment conditions that would result in the formation of a plasma with ionic species concentrations easily relatable to the relative abundance of elements in the original material while simultaneously minimizing the initial ion kinetic energies to the point where time of flight analysis could be used to reconstruct the ion spectra without undue requirements on the electronics system. It was found that reasonably uniform ion representation in the plasma could not be obtained except for bombardment conditions leading to high plasma temperatures with relatively large values of ion kinetic energies resulting. Fortunately, the concept of "energy-time" focus was discovered. Not only does energy-time focus minimize the effects of the broad range of ion energies inherent in the plasma, it dramatically increases the overall ion flight time to the ion detector for a given value of ion accelerating voltage. This will decrease the required speed of the analog-to-digital converter system to a much more easily attainable value.

We also found that the laser pulse energy required is only on the order of one millijoule or less. In fact, it must be small to reduce the ion current in the accelerating region below the space charge limitation. The laser must be of reasonably good beam quality with a focal spot in the ten to one hundred micron range. The pulse duration must be on the order of 10 ns or less to achieve the required laser beam power at the point of irradiation. All of these parameters appear to be within the state of the art for flight development.

These findings, combined with the results of other workers in the field as described in recent publications, provide strong evidence as to the feasibility of the CPA concept. There are, of course, a number of engineering design problems to be solved and there must be an extension of the present work to more adequately demonstrate the definitive nature of the results that could be expected from a flight experiment. Most of these items have been discussed in a proposal for a follow-on effort to the current program.

APPENDIX

COMETARY PARTICULATE ANALYSIS BY LASER BLOWOFF

# INTRODUCTION

The unambiguous analysis of cometary material collected by a remote probe as to chemical composition and structure is a major technological challenge. Almost without question several analytical techniques which complement each other will be necessary. Since weight and power considerations severely limit the number and type of instruments which can be carried, it will be necessary to choose an optimum array of instruments. It is the purpose of this paper to describe one type of instrument which we believe would supply very valuable capabilities to a cometary rendezvous probe. It is not our intention at this time to argue overall merits of this technique versus others since these will depend on the detailed goals of the mission.

# LASER BLOWOFF MASS ANALYZER

The instrument and technique may be characterized as a "Laser Blowoff Mass Analyzer" (LABMA). In simplest terms the instrument is an ion mass spectrometer whose source of ions consists of a tiny expanding plasma "bubble" of material to be analyzed, produced through vaporization and ionization of a very small volume of the material by a pulsed laser beam focused onto the material. In a generic sense only the ion source is unique to LABMA and in principle it could be attached to any type of ion mass spectrometer. However the inherent very short pulsed nature of the ion source lends itself well to time-of-flight mass analysis with its clear advantage of being almost passive without DC magnetic fields or RF electric fields. For example no source of RF power is needed as with a quadrupole mass spectrometer, and no RF background is produced; no stray DC magnetic fields are produced as with a magnetic deflection mass spectrometer. Furthermore, no "sweeping" over the mass range is necessary since an entire mass spectrum is collected with each laser shot. (It may be noted that these features contrast with Secondary Ion Mass Spectrometry, SIMS, which precludes use of time-of-flight mass spectrometers.) Because of these advantages of the time-of-flight (TOF) mass analyzer, and because

47

TOF appears to be feasible in conjunction with LABMA, the following discussion will assume that LABMA will utilize TOF mass analysis.

The key element in the LABMA method is the production of ions through deposition of laser energy in the sample to be analyzed, causing rapid vaporization and ionization of sample material. The process is very complex and a number of questions about this ion source must be considered.

1. Most importantly, is the ratio of the number of ions produced to the number of atoms in the sample the same for all atomic species regardless of chemical structure?

2. What is the charge state of the ions (single or multiple charge), and to what extent does it depend on species?

3. What is the chemical state of the ions (atomic or molecular), and how does it depend on the chemical structure of the original sample?

4. What is the kinetic energy of the ions as they enter the mass spectrometer?

5. How many ions are produced per laser pulse?

6. What is the time dependence of the ion pulse?

As would be expected the answers to these questions depend on the degree of quantitative accuracy demanded for the measurements. The discussion following will attempt to give reasonable answers. The first three are basic to the analysis method by LABMA, while the latter three are related to the resolution and sensitivity of the TOF mass spectrometer. It is asserted here that for the main atomic species of interest, sufficient evidence will be presented to strongly suggest that useful data can be obtained from LABMA analyses on samples of unknown character, and if it is possible to calibrate with samples resembling the actual cometary particulates to be encountered, results with good accuracy ($\pm$ 20%) should be obtainable. It must be emphasized however that only with thorough studies of a variety of materials with an actual operating LABMA can such a suggestion be validated.

On the other hand, of the analytical methods utilizing a mass spectrometer, which would be essential to obtaining isotopic ratios (e.g. SIMS),

the LABMA source of ions appears least subject to errors due to these questions. A considerable literature [1-4] is available which points out the large (x $10^3$) differences in sensitivity as a function of species and chemical composition encountered in SIMS analyses, as well as the positive attributes of SIMS for certain types of measurements. By contrast, it has been reported by several investigators[5-8] that LABMA-type laser blowoff ion sources are relatively less subject to differences in ionization efficiencies between chemical species, particularly so for metals (to less than x 2).

1. Thus with regard to Question 1 concerning overall detection efficiency for various species, the recent and extensive work[5,6] of a German group is valuable. (This work was brought to our attention by Dr. Jochen Kissel of Max Planck Institute, Heidelberg, who recently spent two months in our laboratory.) In conjunction with the company Leybold-Heraeus they have developed a Laser Microprobe Mass Analyzer, LAMMA. (It is also a LABMA by our definition.) Their LAMMA is designed to laser vaporize, ionize and time-of-flight mass analyze sub-cellular volumes 0.5 µm dia x 0.5 µm thick of biological tissues in order to map species location within cells. The instrument is operating, and proves the feasibility of a LABMA with high resolution (both mass and spatial), high sensitivity, and calibratable detection efficiency even for biological specimens. Cometary particulate analysis, with a far less complex species makeup, should be less demanding.

Reference 6 lists ionization-sensitivities for a number of metals in small concentration in organic films. Except for the alkali metals which have an order of magnitude higher sensitivity, the sensitivities for a variety of metals vary by a factor of x 30 for the Leybold-Heraeus LAMMA configuration. However, the LAMMA configuration is probably not the optimal LABMA for the cometary particulate analyzer for several reasons. First, the laser beam strikes the backside of what is essentially a free standing very thin film; thus "large" (greater than tens of microns thickness) cometary particulates could not be reliably analyzed. Second, it appears that plasma temperatures are low enough to cause the ionization sensitivities to vary markedly because of different ionization potentials;

this is probably also due to the "backside" illumination. The appearance of both positive and negative ions, as well as molecular ions, gives a measure of the temperatures reached in the LAMMA configuration. There is one great advantage to this LAMMA configuration, in that it produces ions with very low (few eV) initial energies (as well as being essential for simultaneous microscopic observation and sampling of biological samples for which it is designed). Low initial energies are essential to adequate mass resolution for TOF mass spectrometers of reasonable size, unless an "energy-time focus" could be utilized. (It is asserted here that such an energy-time focus technique has been discovered, and it will be described later in this paper.) If it is assumed for the moment that initial ion kinetic energy is unimportant, a more appropriate LABMA ion source may be discussed which appears from published data to be almost ideal for cometary particulate analysis. Reference 7 describes such a device which utilizes front-surface illumination, 200 nsec ruby laser pulse, 5 mJ pulses, 200 $\mu$m dia spot, 0.6 $\mu$m depth, and achieves quantitative ($\pm$ 20%) analysis of metals from a variety of alloys and minerals. Although the pulse length is somewhat too long for TOF and the spot size is a bit larger than desired, these parameters are close enough to those desired to suggest that results will still be good with the better parameter values. This must obviously be tested. Eloy[7] was not concerned with initial ion energies since he overwhelmed the initial energy effects with acceleration to high energies followed by magnetic mass analysis and photographic plate detection. The results of Eloy (and less extensive results of our own) suggest that front surface illumination produces higher temperatures on the leading edge of the plasma bubble and therefore, less variation in ionization efficiencies caused by differing ionization potentials, and that quantitative mineral analysis is achievable so long as initial ion energy may be neglected. This initial energy aspect will be discussed further below.

2. The question of the charge state of the ions does not appear to pose major problems, based on the work of the LAMMA group[5,6] and Eloy[7]. The former speak of doubly charged ions being less than $10^{-3}$ abundant, while Eloy speaks of "very small amounts," even at the apparently higher temperatures from front surface illumination. The LAMMA group report

seeing halogens only as negative ions, while Eloy does not mention negative ions.

3. The chemical state of the ions (molecular or atomic) appears to depend on whether front or backside illumination is used. Thus Eloy with frontside illumination, higher temperatures and less dependence on ionization potentials reports no molecular ions. The LAMMA group report organic "fingerprints" of series of organic molecular ions, but indicate the results are very sensitive to laser illumination conditions. If front surface illumination is used, it appears likely that only atomic ions will be significant, and therefore no chemical structure analysis will be possible. On the other hand, reducing the laser power density might give at least qualitative data on molecules, and this should certainly be tested.

4. The question of initial ion kinetic energy is critical if TOF (time-of-flight) mass analysis is to be used. The LAMMA group reports initial energies of a few eV for the backside illumination of organic films, but energies far above 100 eV for metal films. Other groups[8] report initial energies to above 200 eV. Eloy reports no measurement of initial energies, but by comparing his mass spectra using the LABMA-type source versus a spark source, it is possible to infer that his initial energies were up to 100 eV, and appeared to have a roughly Maxwell-Boltzman distribution with kT = 50 eV. Although prohibitively high for a conventional TOF mass spectrometer, this initial energy (or even x 4 higher) can be easily handled by the energy-time focus TOF to be described below. Thus it appears that from the standpoint of initial ion energy, a front surface illumination LABMA is feasible.

5. The number of ions produced per pulse in the Eloy[7] experiments was 2 x 10^{11} ions total per pulse, with about 1/6 of these passing through the spectrometer. This number or more has generally been reported by the other groups. Actually the problem may well be too many ions when the energy time focus technique is applied due to space charge problems. At worst, if space charge becomes a problem, multiple laser shots at lower ion production per shot or neutral filtering of ions could be necessitated. It certainly appears that sufficient ions will be produced per laser shot to analyze the major expected species from cometary particulates.

6. In order to use TOF (time-of-flight) mass analysis, it is necessary to have all ions produced in a time short compared to the difference in ion flight times between the highest adjacent mass peaks of interest. For the TOF to be described below and for mass resolution of 100, maximum allowable ion production times are around 30 nanoseconds. This is easily obtainable with Q-switched lasers which deposit their energy in 10 to 50 nanoseconds. This is consistent with laser pulse lengths used for LAMMA and earlier work[8], but is shorter than Eloy (200 nanoseconds). Although it is expected that shorter pulse lengths would not have changed Eloy's results appreciably, this must be tested.

## REFERENCES

1. W. H. Christie, D. H. Smith, R. E. Eby and J. A. Carter, International Laboratory July/August 1978, International Scientific Communications, Inc., Fairfield, CT 06430.

2. A. Benninghoven, Appl. Phys. 1, 3 (1973).

3. A. Benninghoven, Z. Physik 220, 159 (1969).

4. H. E. Beske, Z. Naturforsch 22a, 459 (1967).

5. F. Hillenkamp, E. Unsöld, R. Kaufmann and R. Nitsche, Appl. Phys. 8, 341 (1975).

6. R. Wechsung, F. Hillenkamp, R. Kaufmann, R. Nitsche, H. Vogt, 1979 Conference Scanning Electron Microscopy, Los Angeles, April 17-21, 1978.

7. J. F. Eloy, Int. J. Mass Spectrom. Ion Phys. 6, 101 (1971).

8. N. C. Fenner and N. R. Daly, Rev. Sci. Instr. 37, 1068 (1966).